Journal of
Medicinal Chemistry

Drug Annotation

Discovery of DS-1971a, a Potent Selective NaV1.7 Inhibitor

Tsuyoshi Shinozuka, HIROYUKI KOBAYASHI, Sayaka Suzuki, Kyosuke Tanaka, Narayan Karanjule, Noriyuki Hayashi, Toshifumi Tsuda, Eri Tokumaru, Masahiro Inoue, Kiyono Ueda, Hiroko Kimoto, Yuki Domon, Sakiko Takahashi, Kazufumi Kubota, Tomihisa Yokoyama, Akiko Shimizugawa, Ryuta Koishi, Chie Fujiwara, Daigo Asano, Tomoko Sakakura, Kiyoshi Takasuna, Yasuyuki Abe, Toshiyuki Watanabe, and Yutaka Kitano

J. Med. Chem., **Just Accepted Manuscript** • DOI: 10.1021/acs.jmedchem.0c00259 • Publication Date (Web): 11 May 2020

Just Accepted

is published by the American Chemical Society. 1155 Sixteenth Street N.W., Washington, DC 20036

Discovery of DS-1971a, a Potent Selective $Na_V1.7$ Inhibitor

Tsuyoshi Shinozuka,,† Hiroyuki Kobayashi,† Sayaka Suzuki,† Kyosuke Tanaka,† Narayan Karanjule,† Noriyuki Hayashi,† Toshifumi Tsuda,† Eri Tokumaru,† Masahiro Inoue,† Kiyono Ueda,‡ Hiroko Kimoto,† Yuki Domon,† Sakiko Takahashi,† Kazufumi Kubota,† Tomihisa Yokoyama,† Akiko Shimizugawa,† Ryuta Koishi,‡ Chie Fujiwara,† Daigo Asano,† Tomoko Sakakura,† Kiyoshi Takasuna,† Yasuyuki Abe,† Toshiyuki Watanabe,† and Yutaka Kitano†*

†R&D Division, Daiichi Sankyo Co., Ltd., 1-2-58 Hiromachi, Shinagawa-ku, Tokyo 140-8710, Japan

‡R&D Division, Daiichi Sankyo RD Novare Co., Ltd., 1-16-13 Kitakasai, Edogawa-ku, Tokyo 134-8630, Japan

ABSTRACT

A highly potent, selective $Na_V1.7$ inhibitor, DS-1971a has been discovered. Exploration of the left-hand phenyl ring of sulfonamide derivatives (**I** and **II**) led to the discovery of novel series of cycloalkane derivatives with high $Na_V1.7$ inhibitory potency in vitro. As the right-hand heteroaromatic ring affected the mechanism-based inhibition liability of CYP3A4, replacement of this moiety resulted in the generation of 4-pyrimidyl derivatives. Additionally, GSH adducts formation, which can cause idiosyncratic drug toxicity, was successfully avoided by this modification. An additional optimization led to the discovery of DS-1971a. In preclinical studies, DS-1971a demonstrated highly potent selective in vitro profile with robust efficacy in vivo. DS-1971a exhibited a favorable toxicological profile, which enabled multiple-dose studies of up to 600 mg bid or 400 mg tid (1200 mg/day) administered for 14 days

to healthy human males. DS-1971a is expected to exert potent efficacy in patients with peripheral neuropathic pain, with a favorable safety profile.

INTRODUCTION

Humans experience pain via nociceptive stimuli, such as tissue damage, whereas other types of pain without meaningful stimulation are often more problematic; this type of pain is termed neuropathic pain (NP). A variety of pathological conditions, including viral infection, spinal cord injury, and diabetes, are known to induce NP via dysfunction or lesions in the nervous system.[1] The typical symptoms of NP are spontaneous pain, hyperalgesia, and allodynia, and the duration of such symptoms vary. Peripheral neuropathic pain (PNP) is a debilitating condition that affects patients spontaneously, and is one of the most common types of NP.[2] Although NP and PNP are not lethal conditions, they affect the quality of life (QOL) of patients. There are several medications approved for the treatment of such pain, including calcium channel $\alpha_2\delta$ ligands, tricyclic depressants, and sodium channel blockers. However, there remain substantial unmet medical needs for the treatment of PNP, including diabetic neuropathic pain (DNP), and patients continue to demand potent analgesic drugs with few adverse effects.[3,4]

Voltage-gated sodium channels (Na_Vs) play a predominant role in the conduction of action potentials in the nervous system. A gain of function mutation in the SCN9A gene, which encodes $Na_V1.7$, leads to extremely painful disorders, such as paroxysmal extreme pain disorder (PEPD) and peripheral erythromelalgia (PE).[5,6,7] Conversely, loss of function of the SCN9A gene was shown to result in a rare genetic condition called congenital insensitivity to pain (CIP).[8,9] Patients with CIP present a normal phenotype, similar to healthy individuals, except for anosmia, which is a lack of olfactory function.[9] Deletion of the SCN9A gene in mice, in both sensory and sympathetic neurons was reported to result in the same phenotype observed in humans.[10] Thus, genetic evidence suggests that selective inhibition of $Na_V1.7$ may have potential as a potent analgesic drug with a high safety index. In particular, selective $Na_V1.7$ inhibition is expected to demonstrate a high safety margin with regards the central nervous system

(CNS), owing to the predominant expression of the $Na_V1.7$ isoform in the peripheral nervous system (PNS).[11] CNS adverse effects often lead to treatment interruptions with calcium channel $\alpha_2\delta$ ligands.[12]

High subtype selectivity is crucial for $Na_V1.7$ inhibitors, because the inhibition of several Na_Vs results in adverse effects. $Na_V1.1$ is expressed in CNS, and the inhibition of $Na_V1.1$ leads to CNS adverse effects. Furthermore, given that $Na_V1.5$ is highly expressed in cardiac myocytes, its inhibition can induce adverse cardiovascular (CV) effects.[13] In fact, systemic exposure to non-selective local anesthetic Na_V blockers has been associated with several CNS or CV adverse effects, which limits the use of such drugs.[14]

During the course of our research that aimed to acquire novel analgesic agents,[15] we focused on a highly potent and subtype-selective $Na_V1.7$ inhibitor **I** and **II** reported by the Pfizer group (Figure 1).[16] We hypothesized that the derivatization of these compounds would provide an opportunity to obtain an effective analgesic drug. After the discovery of aryl sulfonamide **II**, numerous analogs were subsequently reported.[17] Herein, we describe the discovery of the clinical compound DS-1971a, which showed ideal analgesic characteristics in preclinical studies. On the basis of our observations that DS-1971a successfully shows a 10-fold higher potency than compound **II** using animal models of neuropathic pain, we believe that DS-1971a has the potential to produce positive results in clinical trials on neuropathic patients.[18]

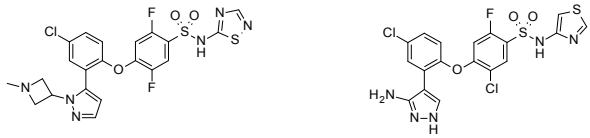

I
hNaV1.1 IC_{50}>100000 nM
hNaV1.5 IC_{50}> 75000 nM
hNaV1.7 IC_{50}: 1.9 nM
mNaV1.7 IC_{50}: 0.55 nM

II (PF-05089771)
hNaV1.1 IC_{50}>100000 nM
hNaV1.5 IC_{50}> 100000 nM
hNaV1.7 IC_{50}: 13 nM
mNaV1.7 IC_{50}: 4.9 nM

Figure 1. The structure of **I** and clinical compound **II** disclosed by the Pfizer group.

RESULTS and DISCUSSION

Chemical Synthesis.

$Na_V1.7$ inhibitors **6** were synthesized as shown in Scheme 1. Sulfonamide **3** was prepared from protected amine **2**. Synthesis of 4-pyrimidine intermediate **3** proceeded smoothly when DABCO was used

as a base, whereas LiHMDS was used to prepare 2-thiadiazole analogs **3**. Boc-protected intermediates were used to synthesize the 4-thiazole analog *rac*-**6f** (structures not shown).[16b] An epoxide-opening reaction with methyl pyrazole yielded racemic alcohol *rac*-**4**. Linear alcohol **4a**, to prepare **6a** (Table 1), was synthesized in the same manner (structures not shown). Compound **4** was exposed to SNAr reaction with **3** to provide *rac*-**5**. Final deprotection yielded $Na_V1.7$ inhibitor *rac*-**6**.

Scheme 1. Synthesis and Chemical Structures of $Na_V1.7$ Inhibitor 6.[a]

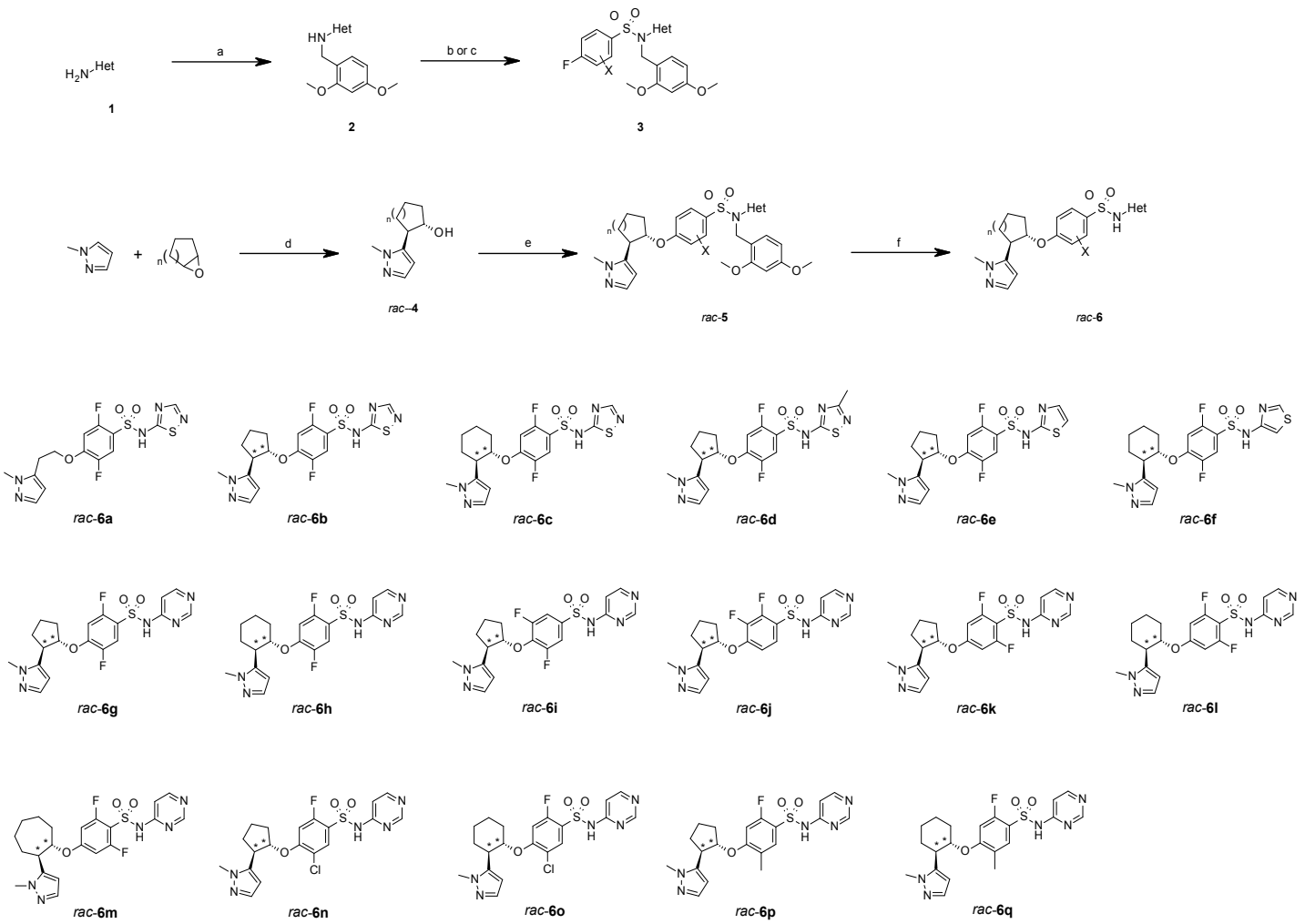

[a]Reagents and conditions: (a) 2,4-dimethoxybenzaldehyde, piperidine, toluene, reflux then $NaBH(OAc)_3$, EtOH; (b) sulfonyl chloride, LiHMDS, THF, -78°C; (c) sulfonyl chloride, DABCO, THF, 0°C; (d) *n*-BuLi, TMEDA, THF, −78°C; (e) **3**, NaH, DMF or DMSO; (f) Et_3SiH, TFA, CH_2Cl_2.

In Vitro Activity and in Vitro ADME Profile.

Initial efforts to modify the sulfonamide moiety were unsuccessful (data not shown). Consequently, we aimed to modify the left-hand phenyl ring, which appeared to be the spacer connecting the benzene sulfonamide moiety and the pyrazole ring.[19] This hypothesis led us to synthesize ethylene compound **6a**, which presented modest $hNa_V1.7$ activity with poor $mNa_V1.7$ potency (Table 1). Accordingly, derivatization of **6a** was initiated to enhance human and mouse $Na_V1.7$ activity. As the introduction of substituents on the ethylene linker led to poor results (data not shown), cycloalkane analogs were prepared. When cyclopentane *rac*-**6b** and cyclohexane *rac*-**6c** were synthesized, both compounds showed excellent $hNa_V1.7$ potency, with high subtype selectivity over $hNa_V1.1$ and $hNa_V1.5$. Moreover, both compounds improved $mNa_V1.7$ activity. Cyclohexane analog *rac*-**6c** demonstrated 10-fold higher $mNa_V1.7$ potency than cyclopentane *rac*-**6b**. Consequently, further optimizations were performed to acquire clinical candidates.

Table 1. In Vitro Profile of **6**[a]

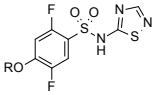

	R	$hNa_V1.1$ IC_{50} (nM)	$hNa_V1.5$ IC_{50} (nM)	$hNa_V1.7$ IC_{50} (nM)	$mNa_V1.7$ IC_{50} (nM)
I		>100000	75000	1.9	0.55
II		>100000	>100000	13	4.9
6a	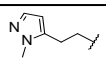	>100000	>100000	800	35300
rac-**6b**		26000	28000	17	240
rac-**6c**	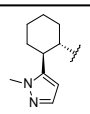	>100000	40000	12	17

[a]Data were obtained using a high-throughput electrophysiology system (IonWorks Quattro). Values are from a single experiment run in quadruplicate.

As shown in Table 2, in vitro ADME profiling revealed that thiadiazoles *rac*-**6b** and *rac*-**6c** possessed high solubility and adequate stability against mice liver microsomes (MLM), whereas both compounds presented poor membrane permeability and inhibited CYP enzymes. Inhibition of CYP enzymes was evaluated at 10 μM, and the mean inhibition (%) was determined. As *rac*-**6b** and *rac*-**6c** showed excellent selectivity with respect to other ion channels, such as $hNa_V1.1$, $hNa_V1.5$, and hERG, the avoidance of CYP inhibition was examined by modifying the right-hand heteroaromatic group.[17h]

When methyl group was introduced to the thiadiazole ring, $hNa_V1.7$ activity was lost (*rac*-**6d**). Although *rac*-**6d** showed no CYP3A4 inhibition, CYP2C9 inhibitory activity was retained. Replacement with 4-oxazole, 2-(1,3,4-thiadiazole), or 3-isoxazole yielded compounds with diminished $hNa_V1.7$ potency (IC_{50} = 3.3, 1.7, and 24.2 μM , respectively). 2-Thiazole *rac*-**6e** maintained potent $hNa_V1.7$ activity, whereas *rac*-**6e** showed mechanism-based inhibition (MBI) of CYP3A4 enzyme. The MBI potency of CYP 3A4 was evaluated by reacting the percent remaining activity at 10 μM with CYP3A4 probe substrates after 0.5 h preincubation in human liver microsomes (HLM). Compound *rac*-**6e** reduced the remaining CYP3A4 activity to 41%. Potent CYP2C9 inhibition was also confirmed for *rac*-**6e**. Introducing 4-thiazole group weakened the results. 4-Thiazole *rac*-**6f** demonstrated GSH adduct formation in HLMs in a GSH-trapping assay. GSH adduct formation is often associated with idiosyncratic drug toxicity (IDT), which has led to the withdrawal of many drugs from the market.[20] Both thiazoles *rac*-**6e** and *rac*-**6f** showed diminished microsomal stability owing to higher lipophilicity. In contrast, molecules with 4-pyrimidine avoided not only GSH adduct formation but also MBI liability (compounds *rac*-**6g** and *rac*-**6h**). Thus, such limitations may be controlled by a right-hand heteroaromatic ring. Further optimization supported this hypothesis, as none of 4-pyrimidine-based sulfonamide analogs synthesized were associated with these issues. The fair membrane permeability was observed in 4-pyrimidines *rac*-**6g** and *rac*-**6h**. Although 4-pyrimidines *rac*-**6g** and *rac*-**6h** successfully avoided the aforementioned issues, both compounds diminished human and mouse $Na_V1.7$ activities by several folds, and still inhibited CYP2C9 and CYP3A4. Further derivatization was required to enhance in vitro potency and prevent CYP inhibition.

Table 2. $Na_V1.7$ Potency and In Vitro ADME Profiles of **6**

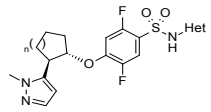

	Het	n	hNa$_V$1.1 IC$_{50}$ (nM) [a]	hNa$_V$1.5 IC$_{50}$ (nM) [a]	hNa$_V$1.7 IC$_{50}$ (nM) [a]	mNa$_V$1.7 IC$_{50}$ (nM) [a]	hERG IC$_{50}$ (nM) [a]	Log D [b]	PAMPA P_{app} (10^{-6} cm/s) [c]	Solubility (nM) [d]	MS (%) Mouse [e]	DI (%, 2C9) [f]	DI (%, 3A4) [f]	MBI [g]	GSH adduct formation [h]
rac-**6b**		1	26000	28000	17	240	>100000	0.6	0.3	>1900	91	93	97	NT	Negative
rac-**6c**		2	>100000	40000	12	17	>100000	0.7	0.3	>2000	75	87.4	>90	NT	NT
rac-**6d**		1	>100000	>100000	56100	NT	>100000	0.9	12.6	1800	69	89.2	17.2	102.4	Negative
rac-**6e**		1	13000	63000	28	100	>100000	2.1	>50	250	54	>90	0	41.2	Negative
rac-**6f**		2	91000	>100000	290 ± 0 [i]	2800 ± 500 [i]	94000	1.8	>50	660	28	66.2	75.1	11.6	Positive
rac-**6g**		1	>100000	>100000	180 ± 30 [i]	1300	>100000	0.3	7.1	740	100	86.3	35.3	119.7	Negative
rac-**6h**		2	>100000	>100000	113 ± 18 [i]	400	>100000	0.3	5.0	1900	80	76	50.4	81.0	Negative

[a]Data were obtained with a high-throughput electrophysiology system (IonWorks Quattro). Values are from a single experiment run in quadruplicate. [b]Distribution coefficients (Log D) were measured after partition between 1-octanol and PBS (pH = 7.4). [c]Parallel artificial membrane permeation assay (PAMPA) was performed at pH 7.4. [d]Aqueous thermodynamic solubility at pH 6.8. [e]Mouse microsomal stability was assessed based on test compound (%) remaining after 0.5 h of incubation with MLM. [f]Inhibition (%) of CYP enzymes at 10 μM. [g]The % remaining activity at 10 μM reacted with CYP3A4 probe substrates after 0.5 h preincubation in HLM. [h]GSH-trapping assay in HLM at 0.5 mM. [i]Values represent at least two independent experiments run in quadruplicate. Each value represents the mean ± standard error of the mean (S.E.M).

The introduction of substituents on the central benzene ring was subsequently investigated (Table 3). Given that 2-fluoro or 3-fluoro derivatives did not show high $Na_V1.7$ potency in vitro (IC_{50} = 0.47, 1.7 μM, respectively), difluoro-substituted analogs were synthesized. 3,5-Difluoro analog *rac*-**6i** was found

to have lost $hNa_V1.7$ activity, whereas 2,3-difluoro analog *rac*-**6j** showed diminished activity. Among difluoro-substituted compounds, 2,6-difluoro derivative *rac*-**6k** showed high potency against human and mouse $Na_V1.7$ in vitro with diminished CYP3A4 liability. When the saturated ring size of *rac*-**6k** was modified, cyclohexane *rac*-**6l** enhanced $Na_V1.7$ activities by approximately two fold. Cyclohexane *rac*-**6l** also maintained an acceptable in vitro ADME profile with modest CYP inhibition. Although potent $Na_V1.7$ activities were observed in cycloheptane *rac*-**6m**, *rac*-**6m** displayed diminished selectivity with respect to $hNa_V1.1$ and $hNa_V1.5$. Thus, saturated ring was fixed to cyclopentane or cyclohexane for further modification. Although 2-fluoro-5-chloro analog *rac*-**6n** displayed high in vitro potency against both species, potent CYP2C9 inhibition remained an issue. Six-membered analog *rac*-**6o** showed high $Na_V1.7$ potency as well as modest CYP3A4 liability. Similar SAR results were obtained in 2-fluoro-5-methyl derivatives *rac*-**6p** and *rac*-**6q** to identify *rac*-**6p** with potent activity and an acceptable in vitro ADME profile.

On the basis of Na_V activities combined with in vitro ADME profile, *rac*-**6l**, *rac*-**6o**, and *rac*-**6p** were selected for an evaluation of thermal hyperalgesia using Seltzer (partial sciatic nerve ligation [PSL])[21] model mice (*vide infra*) ($n = 4$); *rac*-**6o** was found to be the most potent of the three compounds, and thus was selected for further pharmacological evaluation.[22]

Table 3. $Na_V1.7$ Potency and In Vitro ADME Profiles of **6**

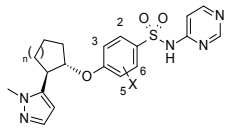

	n	X	hNa_V 1.1 IC_{50} (nM)[a]	hNa_V 1.5 IC_{50} (nM)[a]	hNa_V 1.7 IC_{50} (nM)[a]	mNa_V 1.7 IC_{50} (nM)[a]	hERG IC_{50} (nM)[a]	Log D[b]	PAMPA P_{app} (10^{-6} cm/s)[c]	Solubility (nM)[d]	MS (%) Mouse[e]	DI (%, 2C9)[f]	DI (%, 3A4)[f]
rac-**6g**	1	2-F, 5-F	>100 000	>100 000	180 ± 30[g]	1300	>100 000	0.3	7.1	740	100	86.3	35.3

rac-**6i**	1	3-F, 5-F	>100 000	NT	>100 000	NT	NT	NT	NT	NT	NT	NT	NT
rac-**6j**	1	2-F, 3-F	>100 000	84000	495 ± 35[g]	2800	>100 000	0.4	5.4	550	82	>90	60.3
rac-**6k**	1	2-F, 6-F	52000	>100 000	60 ± 23[g]	96	>100 000	0.1	2.2	1800	80	75	22.7
rac-**6l**	2	2-F, 6-F	>100 000	>100 000	30	56	>100 000	0.1	2.2	1800	77	65.9	45.2
rac-**6m**	3	2-F, 6-F	14000	96000	28	41	>100 000	0.6	6.7	1040	97	80.4	53.9
rac-**6n**	1	2-F, 5-Cl	>100 000	>100 000	45	28	>100 000	0.9	14.3	240	88	>90	53.3
rac-**6o**	2	2-F, 5-Cl	>100 000	>100 000	24.5 ± 8.5[g]	26.5 ± 14.5[g]	>100 000	0.8	6.3	>2000	70	86.8	56.6
6o	2	2-F, 5-Cl	>100 000	93000	21.7 ± 4.4[g]	56.3 ± 6.4[g]	>100 000	0.8	5.2	1500	92	70.0	59.5
rac-**6p**	1	2-F, 5-Me	92000	>100 000	24	28	>100 000	0.9	10.3	1200	87	79.8	42.8
rac-**6q**	2	2-F, 5-Me	16000	>100 000	31	15	90000	0.9	6.7	1800	75	70.6	52.7

[a]Data were obtained with a high-throughput electrophysiology system (IonWorks Quattro). Values are from a single experiment run in quadruplicate. [b]Distribution coefficients (Log D) were measured after partition between 1-octanol and PBS (pH = 7.4). [c]Parallel artificial membrane permeation assay (PAMPA) was performed at pH 7.4. [d]Aqueous thermodynamic solubility at pH 6.8. [e]Mouse microsomal stability was assessed based on test compound (%) remaining after 0.5 h of incubation with MLM. [f]Inhibition (%) of CYP enzymes at 10 μM. [g]Values represent at least two independent experiments run in quadruplicate. Each value represents the mean ± S.E.M.

Preparation of DS-1971a.

Prior to pharmacological assessments, the chiral form of *rac*-**6o** was synthesized. The optical resolution of racemic alcohol *rac*-**4o** (*n* = 2, Scheme 1) was achieved using CHIRALPAK IB, followed by manipulations to obtain **6o** (DS-1971a). The stereochemistry of DS-1971a was determined by X-ray crystallographic analysis (Figure 2). This synthetic scheme was able to generate DS-1971a at over 200 g. Note that enantiomer *ent*-**6o** lost potent $hNa_V1.7$ potency (IC_{50}: 47 μM against $hNa_V1.7$). As indicated in Table 4, compound **6o** showed $Na_V1.7$ activity and an in vitro ADME profile comparable to those of *rac*-**6o**.

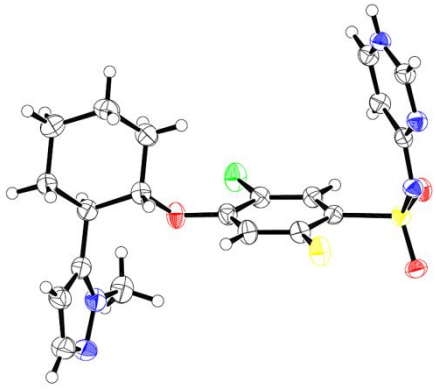

Figure 2. An ORTEP view of DS-1971a (CCDC ID: 1989861).

In Vitro Profile of DS-1971a.

The whole-cell manual patch-clamp method was employed to investigate the effects of DS-1971a on the peak currents of several Na_Vs, as shown in Table 4. DS-1971a inhibited human and mouse $Na_V1.7$ with IC_{50}s 22.8 and 59.4 nM, respectively. Weak inhibitory activity was observed against $hNa_V1.2$ and $hNa_V1.6$. DS-1971a possessed superior selectivity against $hNa_V1.1$ and $hNa_V1.5$, because the IC_{50}s of both $hNa_V1.1$ and $hNa_V1.5$ exceeded 100 μM. The effect of DS-1971a on the potassium currents through hERG was evaluated via the whole-cell manual patch-clamp method (Table 4). The rates of inhibition with 10, 30, and 100 μM of DS-1971a were 2.4, 2.9, and 23.5%, respectively. Thus, DS-1971a demonstrated low inhibitory activity against the hERG channel. In vitro pharmacological activity of DS-1971a against 67 receptors, channels, and transporters was evaluated by radioligand binding assays at 10 μM to confirm the absence of significant responses (≥ 50% inhibition).[23] These data clearly indicated that DS-1971a is a highly potent selective $Na_V1.7$ inhibitor in vitro.

Table 4. In Vitro Profile of DS-1971a[a]

	% Inhibition at 100 μM	IC_{50} (nM) (95% CI)
$hNa_V1.1$[b]	10.53 ± 4.24	>100000
$hNa_V1.2$[b]	75.40 ± 7.07[d]	1960

		(1010-3820)
$hNa_V1.3^b$	-0.76 ± 7.45	>100000
$hNa_V1.4^b$	5.00 ± 3.98	>100000
$hNa_V1.5^b$	-23.91 ± 2.22	>100000
$hNa_V1.6^b$	86.49 ± 5.81[e]	475 (190-1190)
$hNa_V1.7^b$	95.43 ± 4.25[f]	22.8 (18.4-28.2)
$hNa_V1.8^b$	0.35 ± 7.25	>100000
$mNa_V1.1^b$	10.39 ± 3.89	>100000
$mNa_V1.5^b$	-2.51 ± 1.18	>100000
$mNa_V1.7^b$	81.90 ± 0.84[f]	59.4 (25.7-137)
hERG[c]	23.5 ± 2.69	>100000

[a]Data were obtained via the whole-cell manual patch clamp method. Each value represents the mean ± S.E.M. [b]$n = 3$. [c]$n = 4$. [d]%Inhibition at 10 μM. [e]%Inhibition at 3 μM. [f]%Inhibition at 0.3 μM.

Blocking Kinetics of $Na_V1.7$ Channel Current by DS-1971a.

DS-1971a demonstrated potent and selective inhibition of $Na_V1.7$, as well as unique blocking kinetics. The blocking kinetics of DS-1971a were evaluated using a manual patch-clamp method. Cells expressing $hNa_V1.7$ or $mNa_V1.7$ were clamped from the prepulse potential of −50 mV for 9 s to the hyperpolarizing potential of −120 mV for 1 s to reprime channels not bound by compounds, and then given a 10 ms test pulse to −10 mV to elicit current. The voltage pulses were run continuously for 20 min (10 min with perfusion of the test article, and 10 min following washout). A nonselective Na_V blocker, mexiletine, was used as a control. The time course of $hNa_V1.7$ inhibition by DS-1971a is presented in Figure 3A. While mexiletine inhibited $hNa_V1.7$ within a few seconds, DS-1971a induced a slower onset of inhibition In contrast, the dissociation velocity of DS-1971a was slower than that of mexiletine. These unique blocking kinetics were observed when $mNa_V1.7$ was utilized (Figure 3B). The association and dissociation

velocities of DS-1971a for human $Na_V1.7$ were slower than those of mice orthologues. The dissociation half-lives of DS-171a were estimated as 14 min for $hNa_V1.7$ and 2.8 min for $mNa_V1.7$. Thus, DS-1971a showed unique blocking kinetics with $Na_V1.7$, which are expected to result in high in vivo efficacy due to the longer residence time; in vivo studies (*vide infra*) are required to support this.

A) B)

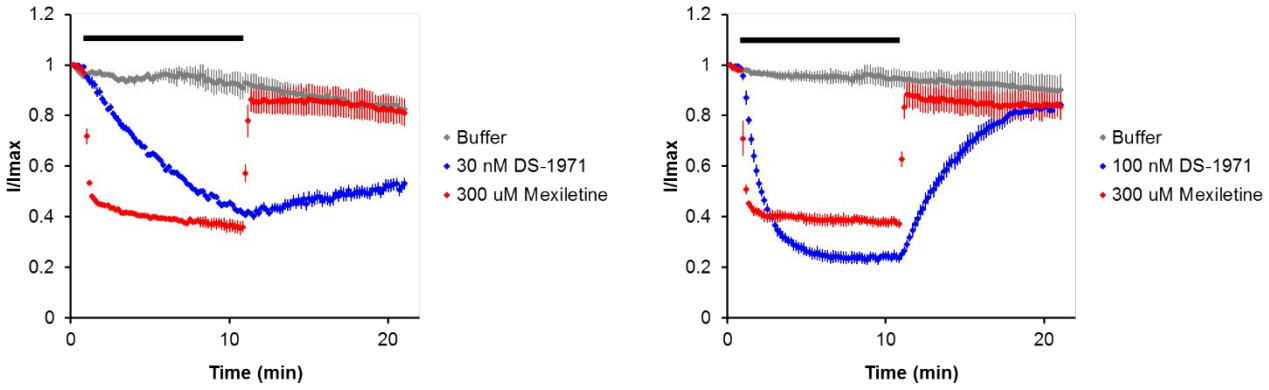

Figure 3. Blocking kinetics of $Na_V1.7$ channel current by DS-1971a (A: $hNa_V1.7$, B: $mNa_V1.7$). Data represent the mean ± S.E.M. (n = 3 or 4).

Effect of DS-1971a on Mechanical Hypersensitivity.

The in vivo pharmacological effects of DS-1971a on mechanical hypersensitivity were investigated using Chung (spinal nerve ligation [SNL])[24] and PSL model mice, as shown in Figure 4. DS-1971a (1, 10, and 100 mg/kg) was administered orally, and the pain threshold in the hind paw was measured with an electronic von Frey anesthesiometer (n = 8). In the SNL model, the pain threshold was significantly (p < 0.01) lowered in model animals, indicating the development of a neuropathic pain state (Figure 4A). The administration of DS-1971a at 1 mg/kg mitigated the pain threshold (p < 0.01) at 60 and 120 min, and this effect lasted until 180 min. The peak efficacy was observed at 120 min. Further mitigation of pain threshold was observed in animals administered 10 mg/kg, and this effect was significant until 180 min (p < 0.01). Maximum efficacy was observed in the animals administered 100 mg/kg; this does

significantly improved the pain threshold to pre-procedure levels ($p < 0.01$) at 120 and 180 min. This potent effect was significant until 240 min ($p < 0.01$). To calculate total analgesic efficacy, the $AUC_{0\text{-}4\ h}$ of each curve presented in Figure 4A was calculated. As depicted in Figure 4B, there was a clear dose-dependent suppression of the pain threshold, and a significant ($p < 0.01$) improvement of total analgesic efficacy with all doses. The plasma exposure of DS-1971a at 1 and 3 mg/kg was confirmed through PK studies with mice (*vide infra*).

The mechanical hypersensitivity of PSL mice was then investigated. As shown in Figure 4C and 4D, the results obtained with PSL mice were comparable to those obtained with SNL mice: the pain threshold was mitigated in a clear dose-dependent manner. Notably, a significant ($p < 0.01$) effect was observed for up to 240 min in PSL mice administered 100 mg/kg (Figure 4C).

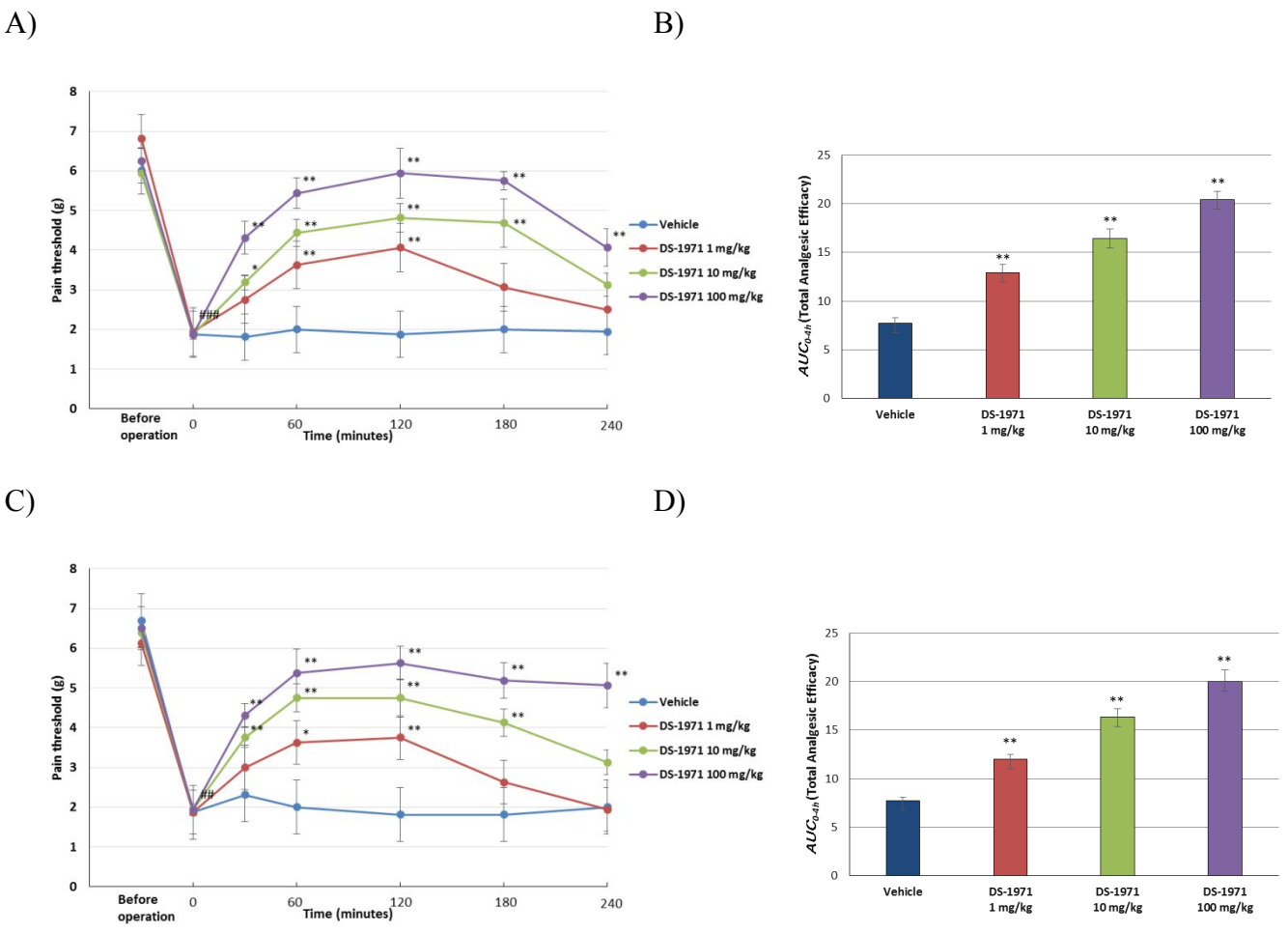

Figure 4. Effect of DS-1971a on mechanical hypersensitivity in SNL (A, B) and PSL (C, D) mice models. The suppression of mechanical hyperalgesia was investigated following oral administration of DS-1971a

in 0.5% methylcellulose (MC) (n = 8). A) Time course of pain threshold (g) following administration of a single dose of DS-1971a (1, 10, and 100 mg/kg) in SNL model mice. B) $AUC_{0\text{-}4\ h}$ (area under the curve of pain threshold in Figure 4A). C) Time course of pain threshold (g) following administration of a single dose of DS-1971a (1, 10, and 100 mg/kg) in PSL model mice. D) $AUC_{0\text{-}6\ h}$ in Figure 4C. Data are presented as the mean ± S.E.M. Statistical significance compared with vehicle treatment is denoted by *($p < 0.05$), **($p < 0.01$), as determined by the Dunnett multiple comparison test. Statistical significance compared with the pre-operation value is denoted by $^{\#\#}$($p < 0.01$) as determined by the paired t-test.

Effect of DS-1971a on thermal hyperalgesia

The effect of DS-1971a on thermal hyperalgesia was investigated using PSL mice (Figure 5). DS-1971a (0.1, 0.3, and 1 mg/kg) was administered orally, and the pain threshold in the hind paw was measured 30, 60, 120, 180, and 240 min after administration using a paw thermal stimulator (n = 8). Compared with the normal control group, the pain threshold was significantly lowered in the model control group, indicating the development of hyperalgesia. As shown in Figure 5A, normal mice withdrew their paw after approximately 10 s, whereas hyperalgesia-induced PSL mice withdrew their paws after approximately 3 s. When DS-1971a was administered at 1 mg/kg, the analgesic efficacy peaked at 60 min, and the pain threshold was significantly improved to the level observed in normal mice ($p < 0.01$). This response lasted up to 120 min, and was lost at 180 min. Similarly, administration of DS-1971a at 0.3 mg/kg significantly lowered the pain threshold from 30 to 120 min ($p < 0.05$ at 30 min, $p < 0.01$ at 60 and 120 min), while administration at 0.1 mg/kg was not effective at lowering the pain threshold. These results clearly indicate that DS-1971a mitigated thermal hyperalgesia in a dose-dependent manner in PSL mice. At the peak efficacy (60 min), there was a significant dose-dependent suppression of thermal hyperalgesia ($p < 0.01$) in 0.3 and 1 mg/kg administered groups. The ED_{50} of DS-1971a at the peak efficacy was 0.32 mg/kg (95% confidence interval: 0.24–0.43 mg/kg). Compound **II** was similarly evaluated for its efficacy against thermal hyperalgesia in PSL mice, and at peak efficacy, it was determined to have ED_{50} of 3.0 mg/kg.[22] Consequently, DS-1971a proved to be 10-fold more potent than compound **II** on a dosage basis.

The efficacy of DS-1971a against a thermal stimulus in PSL mice was found to be more potent than that against a mechanical stimulus. Although the underlying mechanisms remain unclear, these results may reflect the effects mediated via unmyelinated C-fibers. In this regard, it is conceivable that DS-1971a disperses more efficiently in unmyelinated C-fibers than in myelinated A-fibers. This contrasting pattern of DS-1971a distribution in nerve fibers may contribute to difference in the efficacy of impeding thermal and mechanical stimuli. Consistent with this assumption, a higher expression of $Na_V1.7$ in C-fibers than in A-fiber neurons has been reported in rats.[25]

The $AUC_{0\text{-}4\ h}$ of each curve was calculated in order determine total analgesic efficacy. As depicted in Figure 5B, there was a dose-dependent suppression of the pain threshold, and significant ($p < 0.01$) improvements in total analgesic efficacy at 0.3 and 1 mg/kg.

To investigate the therapeutic efficacy at higher dose, DS-1971a (1, 3, and 10 mg/kg) was administered orally to PSL mice ($n = 6$, Figure 5C). Administration of DS-1971a at 10 mg/kg resulted in higher efficacy than 1 mg/kg, which was observed for up to 240 min. Notably, administration of DS-1971a at 10 mg/kg significantly lowered the pain threshold to levels observed in normal mice at 60–180 min ($p < 0.01$). This reduced pain threshold was observed for up to 180 min when DS-1971a was administered at 3 mg/kg. Consequently, a higher dose of DS-1971a improved both the pain threshold and the duration of the therapeutic effect. To assess total analgesic efficacy, the $AUC_{0\text{-}6\ h}$ of each curve in Figure 5C was calculated as indicated in Figure 5D. Significant ($p < 0.01$) improvement in total thermal-evoked pain behavior was confirmed following administration of 3 and 10 mg/kg.

A) B)

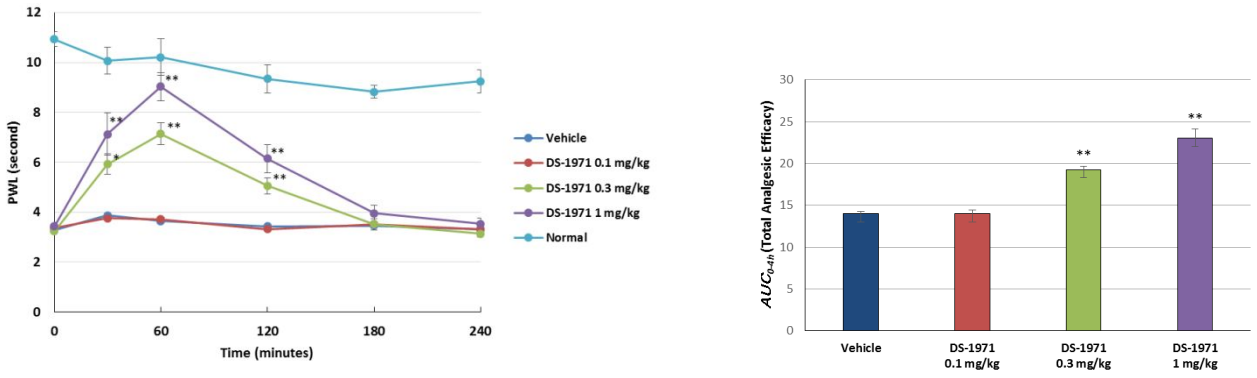

D) E)

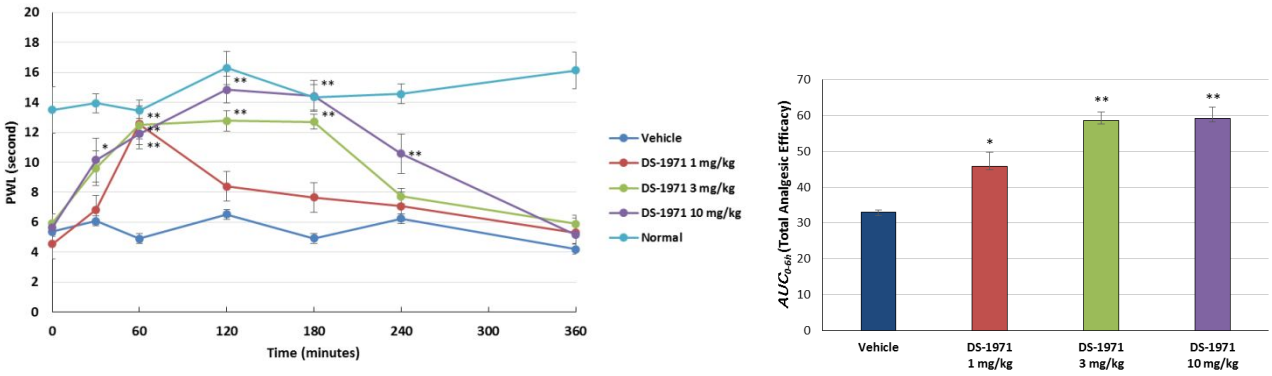

Figure 5. Effect of DS-1971a on thermal hyperalgesia in PSL mice. The suppression of thermal hyperalgesia was investigated following oral administration of DS-1971a in 0.5% MC. A) Time course of paw withdraw latency (PWL, s) following administration of a single dose of DS-1971a (0.1, 0.3, and 1 mg/kg, n = 8). B) $AUC_{0\text{-}4\ h}$ (area under the curve of PWL) in Figure 5A). C) Time course of PWL (s) following administration of a single dose of DS-1971a (1, 3, and 10 mg/kg, n = 6). D) $AUC_{0\text{-}6\ h}$ in Figure 5C. Data are presented as the mean ± S.E.M. Statistical significance compared with vehicle treatment is denoted by *($p < 0.05$), **($p < 0.01$), as determined by the Dunnett multiple comparison test.

ADME and PK Profile of DS-1971a

ADME profiling established that DS-1971a showed high stability against rodent and dog liver microsomes, whereas modest stability was observed in monkey and human microsomes, as indicated in Table 5. DS-1971a binds to plasma proteins in a reasonable degree. Although the compound inhibited CYP3A4 and CYP2C9 at micromolar concentration, a sufficient margin is expected due to the low predicted pharmacologically effective concentrations.

The PK profile was assessed in preclinical studies using four species, as shown in Table 6. DS-1971a exhibited high clearance (CL) in rodents, whereas better CL was observed in non-rodents. A low distribution volume (V_{ss}) was confirmed in preclinical studies in four species. The compound exhibited high oral bioavailability in dogs, whereas modest bioavailability was observed in rodents. Overall, the preclinical profile of DS-1971a in four preclinical species was suitable for proceeding clinical trials.

To investigate the PK/PD correlation, PK studies were performed in mice (1 and 3 mg/kg) (Table 6). The increase in AUC_{inf} was dose-dependent, whereas the $T_{1/2}$ of plasma DS-1971a was similar following administration of 1 and 3 mg/kg. Thus, the duration of effect was correlated with AUC_{inf} in the PK study.

In order to determine the ability of the compound to penetrate into the brain, brain Kp value was assessed. The brain concentration of DS-1971a was determined 30 min after compound administration (1 mg/kg, po), and was found to be below the lower limit of quantification (Kp brain <0.07) (n = 3).

On the basis of the pharmacologically effective dose (ED_{50} = 0.32 mg/kg) combined with C_{max} at 1 mg/kg in mice (105 nM, Table 6) and the assumption of PK linearity, the pharmacologically effective plasma concentration was calculated as EC_{50} = 33.6 nM. If the plasma protein binding ability is considered, free EC_{50} is 1.1 nM. There was a significant disparity between EC_{50} values calculated based on in vivo investigations and in vitro IC_{50} value in mice (59.4 nM, Table 4). One plausible reason for this disparity is the binding kinetics of DS-1971a, as presented in Figure 3. As DS-1971a has a long residence time in $Na_V1.7$, this may contribute to the higher efficacy observed in vivo than that predicted from in vitro IC_{50} and PK studies. In addition to IC_{50}, the dissociation half-life of the target protein is suggested to be an important factor that determines the pharmacological potency in vivo.[26]

Table 5. ADME Profile of DS-1971a

Log D[a]	PAMPA P_{app} (10^{-6} cm/s)[b]	Solubility (nM)[c]	MS (%)[d]				
			Mouse	rat	dog	monkey	human
0.8	5.2	1500	92	94	95	78	66
Plasma protein binding, %				CYP2C9 IC_{50} (μM)		CYP3A4 IC_{50} (μM)	
mouse	rat	monkey	human				
96.6–96.8%	97.7–97.9%	98.9–99.0%	99.1–99.2%	4.9		8.7	

[a]Distribution coefficients (Log D) were measured after partition between 1-octanol and PBS (pH = 7.4). [b]Parallel artificial membrane permeation assay (PAMPA) was performed at pH 7.4. [c]Aqueous thermodynamic solubility at pH 6.8. [d]Microsomal stability was assessed based on test compound (%) remaining after 0.5 h of incubation with corresponding liver microsomes.

Table 6. PK Parameters of DS-1971a[a]

		C_{max} (nM)	T_{max} (h)	$T_{1/2}$ (h)	AUC_{inf} (h·nM)	F (%)	CL (mL/min/kg)	V_{ss} (L/kg)
Monkey[b]	1 mg/kg	1570 ± 648	0.83 ± 0.29	3.69 ± 0.18	2060 ± 923	35 ± 10	6.55 ± 1.62	0.150 ± 0.009
Dog	1 mg/kg	1708 (1790, 1620)[c]	0.50 (0.50, 0.50)[c]	4.0 (3.8, 4.2)[c]	3230 (3630, 2830)[c]	77 (87, 67)[c]	8.7 (8.6, 8.9)[c]	0.57 (0.49, 0.65)[c]
Rat	1 mg/kg	103 ± 40.8[b]	0.50 ± 0.00[b]	0.77 (0.70, 0.85)[c]	103 (127, 81.6)[c]	16 ± 6.5[b]	47 (55, 39)[c]	1.2 (1.4, 1.1)[c]
Mouse[d]	1 mg/kg	105	0.0833	2.02	68.9	15	78.7	1.37
Mouse[d]	3 mg/kg	464	0.250	1.54	277	11	45.3	0.565

[a]See Table 11 for detailed conditions. Total body clearance (*CL*), distribution volume at steady state (*Vss*) and *F* value were calculated following intravenous (1 mg/kg) administration of DS-1971a. Each value represents the mean ± standard deviation (S.D.). [b]$n = 3$. [c]Individual data ($n = 2$). [d]$n = 3$ for each time point. See SI for the individual data.

In Vivo Safety Pharmacology Studies of DS-1971a.

Preclinical safety pharmacology studies were performed using mice and cynomolgus monkeys. As shown in Table 7, DS-1971a did not exert any notable effects up to 1000 mg/kg in mice or cynomolgus monkeys. Furthermore, on the basis on modified Irwin's multiple observations, spontaneous locomotor activity, and motor coordination via a rota-rod test, DS-1971a did not appear to affect CNS of male mice, or their respiratory system. In conscious and unrestrained male cynomolgus monkeys, DS-1971a had no effects on heart rate, blood pressure (systolic, diastolic, and mean), or electrocardiogram (ECG) parameters (PR interval, QRS duration, QT interval, and QTc) at any evaluated time point. Moreover, no occurrences of arrhythmia were observed. Consequently, a single oral dose of DS-1971a is not considered to affect the cardiovascular system in monkeys at doses up to 1000 mg/kg.

Table 7. In vivo Safety Pharmacology Studies of DS-1971a.

	n	Species	Age	Dose (mg/kg)	NOEL (mg/kg)
Irwin's multiple observation	6	Crl:CD1(ICR) mice	7 weeks	0, 100, 300, 1000	1000
Locomotor activity	8	Crl:CD1(ICR) mice	7 weeks	0, 100, 300, 1000	1000
Motor coordination	8	Crl:CD1(ICR) mice	7 weeks	0, 100, 300, 1000	1000
Respiratory system	8	Crl:CD1(ICR) mice	7 weeks	0, 100, 300, 1000	1000
Cardiovascular system	4	cynomolgus monkeys	5 years	0, 30, 100, 1000	1000

Chronic Toxicity Studies of DS-1971a.

The results of chronic in vivo toxicology studies of DS-1971a are summarized in Table 8. Six- or 9-month repeated dose toxicity studies were conducted in mice (n = 15/sex/group) at 0, 30, 100, and 1000 mg/kg or in cynomolgus monkeys (n = 4/sex/group). In the mouse study, a satellite group was established for the toxicokinetic (TK) evaluation (n = 3 for each blood sampling point), and in the monkey study, additional animals (n = 2/sex) were treated with DS-1971a at a dose level of 1000 mg/kg for 9 months and were withdrawn from treatment to assess the reversibility of any toxicity following a 1-month recovery period. No deaths were noted and no treatment-related changes in clinical signs, body weight, food consumption, ophthalmology, urinalysis, hematology, blood chemistry, necropsy, or histopathology were observed at any doses of both studies including the recovery period. No toxicity was observed up to the highest doses, and the no observed adverse effect level (NOAEL) was considered to be the top dose of 1000 mg/kg/day for both species. In the TK evaluation, the plasma exposure of DS-1971a increased in a dose-dependent manner. Exposure was higher in female mice than in male mice; however, there were no clear sex difference in exposure in monkeys. The TK parameters of the highest doses following the final dosing are shown in Table 8. The pharmacologically effective dose in mice was found to be 0.32 mg/kg. A comparison of exposure at the NOAEL in mice with that at 1 mg/kg (C_{max}: 105 nM, AUC_{inf}: 68.9 h·nM) in the mouse PK study indicates that DS-1971a showed a favorable safety profile in these studies.

This favorable safety profile is consistent the outcome of clinical studies in human, as DS-1971a has been shown to be well tolerated and safe in clinical phase 1 studies. Among these studies, a single ascending dose study using DS-1971a revealed good safety and tolerability up to 1500 mg (https://clinicaltrials.gov/ct2/show/record/NCT02107885), whereas a multiple ascending dose study of up to 600 mg bid or 400 mg tid (1200 mg/day) for 14 days also found DS-1971a to be safe and tolerable (https://clinicaltrials.gov/ct2/show/NCT02190058).

Table 8. Chronic In Vivo Toxicity Study of DS-1971a.

Species	Sex	Duration	Dose (mg/kg)	NOAEL (mg/kg)	TK parameters at final dosing			
					Dose (mg/kg)	C_{max} (nM)	T_{max} (h)	$AUC_{0\text{-}24\ h}$ (h·nM)
Crl:CD1(ICR) mice	Male	6 Months	0, 30, 100, 1000	1000	1000[a]	9440	0.5	65900
Crl:CD1(ICR) mice	Female	6 Months	0, 30, 100, 1000	1000	1000[a]	105000	6.0	1400000
Cynomolgus monkeys	Male	9 Months	0, 10, 100, 1000	1000	1000[b]	28100 ± 14600	1.2 ± 0.4	146000 ±85800
Cynomolgus monkeys	Female	9 Months	0, 10, 100, 1000	1000	1000[b]	22500 ± 14600	1.2 ± 0.4	100000 ± 97200

Each value represents the mean ± S.D. [a]$n = 3$ for each time point. See SI for the individual data. [b]$n = 6$.

CONCLUSIONS

We report the discovery of a highly potent and selective $Na_V1.7$ inhibitor, DS-1971a. Derivatization was focused on the avoidance of issues such as CYP inhibition, MBI, and GSH adduct formation. The finding that the right-hand heteroaromatic ring affects MBI liability and GSH adduct formation led to the discovery of 4-pyrimidiyl derivatives without such liabilities. Further optimizations provided DS-1971a, which inhibited human and mouse $Na_V1.7$ in a highly potent and selective manner. DS-1971a demonstrated unique blocking kinetics on $Na_V1.7$: the onset and recovery from DS-1971a block were

very slow compared with those of mexiletine. In vivo pharmacological profiling revealed that DS-1971a demonstrates potent analgesic efficacy against both thermal and mechanical hypersensitivity induced by nerve ligation. The results of in vivo safety studies (safety pharmacology studies and chronic toxicity studies) revealed no concerns about adverse effects with DS-1971a up to 1000 mg/kg. Although DS-1971a inhibits CYP enzymes, a sufficient margin is expected owing to the low predicted pharmacologically effective concentrations. DS-1971a is expected to be an efficacious analgesic agent with excellent safety profile.

EXPERIMENTAL SECTION

General Procedures.

Starting reagents were purchased from commercial suppliers, and were used without further purification, unless otherwise specified. Chromatographic elution was conducted under continuous monitoring by TLC using silica gel 60F254 (Merck & Co., Inc.) as the stationary phase; and the elution solvent used in column chromatography as the mobile phase. A UV detector was used for detection. Silica gel SK-85 (230–400 mesh) or silica gel SK-34 (70–230 mesh), manufactured by Merck & Co., Inc., or Chromatorex NH (200–350 mesh), manufactured by Fuji Silysia Chemical Ltd., was used as the column-packing silica gel. ^{1}H NMR spectra were obtained on Varian Unity 400 and 500 MHz spectrometers. Spectra were recorded in the indicated solvent at ambient temperature; chemical shifts are reported in ppm (δ) relative to the solvent peak. Resonance patterns are represented with the following notations: br (broad signal), s (singlet), d (doublet), t (triplet), q (quartet), and m (multiplet). MS analysis methods were FAB, EI, or ESI. HRMS was carried out using an LC-MS system composed of a Waters Xevo Quadropole-ToF MS and an Acquity UHPLC system. Elemental analyses were conducted by using a Microcorder JM10 and a Dionex ICS-1500. The purity of compounds was confirmed to exceed 95% by the DAD signal area% performed on an Agilent Infinity 1260 LCMS system. The conditions were as follows: column: Develosil Combi-RP-5 2.0 mmID × 50 mmL, gradient elution: 0.1% HCO_2H-H_2O/0.1%

HCO_2H-MeCN = 98/2 to 0/100 (v/v), flow rate: 1.2 mL/min, UV detection: 254 nm, column temperature: 40°C, ionization: APCI/ESI. All assay compounds were ≥ 95% pure. All in vivo experimental procedures were performed in accordance with the in-house guidelines of the Institutional Animal Care and Use Committee of Daiichi Sankyo Co., Ltd.

General Procedure for Epoxide-Opening Reaction (General Procedure A).

n-Butyllithium (1.63 M solution in hexane; 100 mL, 163 mmol) was added to a solution of 1-methylpyrazole (13.4 g, 163 mmol) in THF (1.0 L) drop-wise at -78°C for 40 min. Epoxide (179 mmol) was then added at −78°C to the reaction mixture, which was subsequently stirred at room temperature for 20 h. A saturated aqueous solution of $NaHCO_3$ (100 mL) was added, and the mixture was extracted several times with EtOAc. The combined organic layers were washed with water, dried over anhydrous Na_2SO_4, and concentrated under reduced pressure. The crude residue was purified by silica gel column chromatography to obtain *rac*-**4**.

General Procedure for S_NAr Reaction to Prepare 9 (General Procedure B).

NaH (2.63 mmol) was added to a solution of protected benzenesulfonamide **3** (1.35 mmol) and alcohol **4** (1.36 mmol) in DMSO or DMF (6.0 mL) at 0°C under N_2, and the mixture was stirred at room temperature for 1 h. Water was added to the cooled mixture, which was then extracted with EtOAc several times. The combined organic layers were washed with water, dried over anhydrous Na_2SO_4, and concentrated under reduced pressure. The crude residue was purified by silica gel column chromatography to obtain compound **5**.

General Procedure for Deprotection (General Procedure C).

The solution of **5** (0.449 mmol), Et_3SiH (0.30 mL), and TFA (3.0 mL) in CH_2Cl_2 (3.0 mL) was stirred at room temperature for 1 h. The reaction mixture was concentrated, and the residue was purified via silica gel chromatography to yield **6**.

General Procedure for Imine Formation, Followed by Reduction (General Procedure D).

A solution of heteroaromatic amine **1** (210 mmol), 2,4-dimethoxybenzaldehyde (69.9 g, 421 mmol), and piperidine (2.08 mL, 21.0 mmol) in toluene (1.0 L) was refluxed with azeotropic removal of water for 7 h. After the cooled reaction mixture was diluted with EtOH (500 mL), $NaBH_4$ (7.96 g, 210 mmol) was added to the mixture at 0°C. After stirring at room temperature for 16 h, water was added, and the mixture was extracted with EtOAc several times. The combined organic layers were washed with water, dried over anhydrous Na_2SO_4, and concentrated under reduced pressure. The crude residue was purified by silica gel column chromatography to obtain compound **2**.

General Procedure for Sulfonamide Formation (General Procedure E).

LiHMDS (1.0 M solution in THF; 4.8 mL, 4.8 mmol) was added to a solution of protected amine **2** (4.00 mmol) in THF (12 mL) dropwise at −78°C. After stirring at −78°C for 10 min, sulfonyl chloride (4.42 mmol) was added at −78°C to the reaction mixture, which was then stirred at room temperature for 2 h. Water was added, and the mixture was extracted with EtOAc several times. The combined organic layers were washed with water, dried over anhydrous Na_2SO_4, and concentrated under reduced pressure. The crude residue was purified by silica gel column chromatography to obtain **3**.

Alternative General Procedure for Sulfonamide Formation (General Procedure F).

Sulfonyl chloride (6.20 mmol) was added to a solution of protected amine **2** (0.76 g, 3.10 mmol) and 1,4-diazabicyclo[2. 2.2]octane (0.70 g, 6.20 mmol) in MeCN (20 mL) at 0°C, which was then was stirred at room temperature for 1 h. After the reaction mixture was filtrated, the residue was concentrated, and the residue was purified with silica gel chromatography to yield compound **3**.

***N*-[(2,4-Dimethoxyphenyl)methyl]-3-methyl-1,2,4-thiadiazol-5-amine (2d)**

Prepared according to General Procedure D. Yield 60%. ^{1}H-NMR (500 MHz, $CDCl_3$) δ 2.36 (3H, s), 3.78 (3H, s), 3.79 (3H, s), 4.29 (2H, d, J = 5.9 Hz), 6.13 (1H, br), 6.40–6.45 (2H, m), 7.15 (1H, d, J = 8.3 Hz).

***N*-[(2,4-Dimethoxyphenyl)methyl]pyrimidin-4-amine (2g)**

Prepared according to General Procedure D. Yield 52%. ^{1}H-NMR (500 MHz, $CDCl_3$) δ 3.80 (3H, s), 3.84 (3H, s), 4.44 (2H, br), 5.33 (1H, br), 6.34 (1H, d, *J* = 5.9 Hz), 6.44 (1H, dd, *J* = 2.4, 8.3 Hz), 6.48 (1H, d, *J* = 2.0 Hz), 7.18 (1H, d, *J* = 8.3 Hz), 8.15 (1H ,d, *J* = 5.4 Hz), 8.55 (1H, s).

***N*-[(2,4-Dimethoxyphenyl)methyl]-2,4,5-trifluoro-*N*-(3-methyl-1,2,4-thiadiazol-5-yl)benzene-1-sulfonamide (3d)**

Prepared according to General Procedure E. Yield 79%. ^{1}H-NMR (500 MHz, $CDCl_3$) δ 2.45 (3H, s), 3.69 (3H, s), 3.73 (3H, s), 5.29 (2H, s), 6.21 (1H, d, *J* = 2.4 Hz), 6.34 (1H, dd, *J* = 2.2, 8.5 Hz), 6.88–6.93 (1H, m), 7.18 (1H, d, *J* = 8.8 Hz), 7.58–7.63 (1H, m).

***N*-[(2,4-Dimethoxyphenyl)methyl]-2,4,5-trifluoro-*N*-(1,3-thiazol-2-yl)benzene-1-sulfonamide (3e)**

Prepared according to General Procedure F. Yield 54%. ^{1}H-NMR (400 MHz, $CDCl_3$) δ 3.73 (3H, s), 3.77 (3H, s), 5.19 (2H, s), 6.36–6.39 (2H, m), 7.01‑7.07 (2H, m), 7.19 (1H, d, *J* = 8.2 Hz), 7.42 (1H, d, J = 3.5 Hz), 7.70‑7.76 (1H, m).

***N*-[(2,4-Dimethoxyphenyl)methyl]-2,4,5-trifluoro-*N*-(pyrimidin-4-yl)benzene-1-sulfonamide (3g)**

Prepared according to General Procedure F. Yield 53%. ^{1}H-NMR (500 MHz, $CDCl_3$) δ 3.78 (3H, s), 3.80 (3H, s), 5.23 (2H, s), 6.42-6.43 (2H, m), 6.99‑7.04 (1H, m), 7.13 (1H, d, *J* = 5.9 Hz), 7.22 (1H, d, *J* = 9.3 Hz), 7.91‑7.96 (1H, m), 8.48 (1H, d, *J* = 6.4 Hz), 8.78 (1H, s).

***N*-[(2,4-Dimethoxyphenyl)methyl]-3,4,5-trifluoro-*N*-(pyrimidin-4-yl)benzene-1-sulfonamide (3i)**

Prepared according to General Procedure F. Yield 39%. ^{1}H-NMR (500 MHz, $CDCl_3$) δ 3.64 (3H, s), 3.76 (3H, s), 5.11 (2H, s), 6.35 (1H, d, *J* = 2.4 Hz), 6.39 (1H, dd, *J* = 2.4, 8.8 Hz), 7.11–7.15 (2H, m), 7.49–7.53 (2H, m), 8.52 (1H, d, *J* = 6.8 Hz), 8.86 (1H, s).

***N*-[(2,4-Dimethoxyphenyl)methyl]-2,3,4-trifluoro-*N*-(pyrimidin-4-yl)benzene-1-sulfonamide (3j)**

Prepared according to General Procedure F. Yield 31%. ^{1}H-NMR (500 MHz, $CDCl_3$) δ 3.78 (3H, s), 3.80 (3H, s), 5.24 (2H, s), 6.42‑6.44 (2H, m), 7.11-7.16 (2H, m), 7.22 (1H, d, *J* = 7.8 Hz), 7.84‑7.89 (1H, m), 8.48 (1H, d, *J* = 5.9 Hz), 8.76 (1H, s).

***N*-[(2,4-Dimethoxyphenyl)methyl]-2,4,6-trifluoro-*N*-(pyrimidin-4-yl)benzene-1-sulfonamide (3k)**

Prepared according to General Procedure F. Yield 18%. ^{1}H-NMR (500 MHz, $CDCl_3$) δ 3.73 (3H, s), 3.78 (3H, s), 5.26 (2H, s), 6.42–6.46 (2H, m), 6.78 (2H, t, *J* = 8.3 Hz), 7.07 (1H, dd, *J* = 1.5, 5.9 Hz), 7.24 (1H, d, *J* = 8.8 Hz), 8.46 (1H, d, *J* = 6.4 Hz), 8.78 (1H, s).

5-Chloro-*N*-[(2,4-dimethoxyphenyl)methyl]-2,4-difluoro-*N*-(pyrimidin-4-yl)benzene-1-sulfonamide (3n)

Prepared according to General Procedure F. Yield 26%. ^{1}H-NMR (500 MHz, $CDCl_3$) δ 3.78 (3H, s), 3.79 (3H, s), 5.23 (2H, s), 6.41–6.43 (2H, m), 6.98 (1H, d, *J* = 9.3 Hz), 7.16 (1H, d, *J* = 7.3 Hz), 7.22 (1H, d, *J* = 8.8 Hz), 8.13 (1H, t, *J* = 7.3 Hz), 8.49 (1H, d, *J* = 5.9 Hz), 8.79 (1H, s).

***N*-[(2,4-Dimethoxyphenyl)methyl]-2,4-difluoro-5-methyl-*N*-(pyrimidin-4-yl)benzene-1-sulfonamide (3p)**

Prepared according to General Procedure F. Yield 79%. ^{1}H-NMR (500 MHz, $CDCl_3$) δ 2.31 (3H, s), 3.77 (3H, s), 3.79 (3H, s), 5.25 (2H, s), 6.40-6.42 (2H, m), 6.83 (1H, t, *J* = 9.3 Hz), 7.20–7.23 (2H, m), 7.89 (1H, t, *J* = 7.8 Hz), 8.45 (1H, d, *J* = 5.9 Hz), 8.77 (1H, s).

2-(1-Methyl-1*H*-pyrazol-5-yl)ethan-1-ol (4a)

Prepared according to General Procedure A. Yield 31%. ^{1}H-NMR (400 MHz, $CDCl_3$) δ 2.92 (2H, t, *J* = 6.7 Hz), 3.84 (3H, s), 3.89-3.93 (2H, m), 6.12 (1H, d, *J* = 2.0 Hz), 7.42 (1H, s).

(1*S,2*R**)-2-(1-Methyl-1*H*-pyrazol-5-yl)cyclopentan-1-ol (*rac*-4b)**

Prepared according to General Procedure A. Yield 21%. ^{1}H-NMR (500 MHz, $CDCl_3$) δ 1.63–-1.91 (4H, m), 2.05-2.12 (1H, m), 2.17-2.24 (1H, m), 3.03 (1H, q, *J* = 8.3 Hz), 3.86 (3H, s), 4.24 (1H, q, *J* = 6.4 Hz), 6.03 (1H, s), 7.39 (1H, s).

(1*S,2*R**)-2-(1-Methyl-1*H*-pyrazol-5-yl)cyclohexan-1-ol (*rac*-4c)**

Prepared according to General Procedure A. Yield 55%. ^{1}H-NMR (400 MHz, $CDCl_3$) δ 1.30-1.48 (4H, m), 1.76–1.91 (4H, m), 2.09–2.15 (1H, m), 2.57-2.63 (1H, m), 3.59–3.65 (1H, m), 3.86 (3H, s), 6.08 (1H, d, *J* = 2.0 Hz), 7.44 (1H, d, *J* = 2.0 Hz).

(1*S,2*R**)-2-(1-Methyl-1*H*-pyrazol-5-yl)cycloheptan-1-ol (*rac*-4m)**

Prepared according to General Procedure A. Yield 13%. ^{1}H-NMR (500 MHz, $CDCl_3$) δ 1.56‑1.89 (9H, m), 1.98‑2.05 (1H, m), 2.76‑2.82 (1H, m), 3.80‑3.86 (1H, m), 3.84 (3H, s), 6.06 (1H, d, *J* = 2.0 Hz), 7.41 (1H, d, *J* = 2.4 Hz).

(1*S*,2*R*)-2-(1-Methyl-1*H*-pyrazol-5-yl)cyclohexan-1-ol (4o)

(1*S**,2*R**)-2-(1-Methyl-1*H*-pyrazol-5-yl)cyclohexan-1-ol **(*rac*-4c)** was optically resolved with CHIRALPAK IB (Daicel Corp.; hexane/ethanol = 9: 1) to yield the title compound as a colorless oil. $[\alpha]^{25}_D$ = 33.3 (*c* 0.916, MeOH).

***N*-[(2,4-Dimethoxyphenyl)methyl]-2,5-difluoro-4-[2-(1-methyl-1*H*-pyrazol-5-yl)ethoxy]-*N*-(1,2,4-thiadiazol-5-yl)benzene-1-sulfonamide (5a)**

Prepared according to General Procedure B. Yield 16%. ^{1}H-NMR (400 MHz, $CDCl_3$) δ 3.21 (2H, t, *J* = 6.3 Hz), 3.73 (6H, s), 3.93 (3H, s), 4.23 (2H, t, *J* = 6.7 Hz), 5.30 (2H, s), 6.15 (1H, d, *J* = 2.0 Hz), 6.25 (1H, d, *J* = 2.0 Hz), 6.36 (1H, dd, *J* = 2.3, 8.6 Hz), 6.59 (1H, dd, *J* = 6.5, 10.8 Hz), 7.19 (1H, d, *J* = 6.7 Hz), 7.44 (1H, d, *J* = 2.0 Hz), 7.55 (1H, dd, *J* = 5.9, 9.8 Hz), 8.20 (1H, s).

***N*-[(2,4-Dimethoxyphenyl)methyl]-2,5-difluoro-4-{[(1*S**,2*R**)-2-(1-methyl-1*H*-pyrazol-5-yl)cyclopentyl]oxy}-*N*-(1,2,4-thiadiazol-5-yl)benzene-1-sulfonamide (*rac*-5b)**

Prepared according to General Procedure B. Yield 51%. ^{1}H-NMR (400 MHz, $CDCl_3$) δ 1.76–1.99 (4H, m), 2.17–2.24 (1H, m), 2.27–2.35 (1H, m), 3.44–3.50 (1H, m), 3.71 (6H, s), 3.87 (3H, s), 4.57–4.61 (1H, m), 5.29 (2H, s), 6.06 (1H, d, *J* = 2.0 Hz), 6.24 (1H, d, *J* = 2.4 Hz), 6.34 (1H, dd, *J* = 2.4, 8.2 Hz), 6.45 (1H, dd, *J* = 6.3, 11.0 Hz), 7.16 (1H, d, *J* = 8.3 Hz), 8.41 (1H, d, *J* = 2.0 Hz), 7.53 (1H, dd, *J* = 6.7, 10.2 Hz), 8.18 (1H, s).

***N*-[(2,4-Dimethoxyphenyl)methyl]-2,5-difluoro-4-{[(1*S**,2*R**)-2-(1-methyl-1*H*-pyrazol-5-yl)cyclohexyl]oxy}-*N*-(1,2,4-thiadiazol-5-yl)benzene-1-sulfonamide (*rac*-5c)**

Prepared according to General Procedure B. Yield 42%. ^{1}H-NMR (400 MHz, $CDCl_3$) δ 1.39–1.70 (4H, m), 1.87–1.90 (1H, m), 1.94–1.98 (1H, m), 2.05–2.09 (1H, m), 2.17–2.21 (1H, m), 2.97–3.03 (1H, m), 3.65 (3H, s), 3.74 (3H, s), 3.90 (3H, s), 4.08 (1H, dt, *J* = 3.9, 10.2 Hz), 5.21 (1H, d, *J* = 15.7 Hz), 5.28 (1H, d, *J* = 15.7 Hz), 6.04 (1H, d, *J* = 2.0 Hz), 6.19 (1H, d, *J* = 2.0 Hz), 6.34 (1H, dd, *J* = 2.4, 8.6 Hz),

6.34-6.39 (1H, m), 7.15 (1H, d, *J* = 8.2 Hz), 7.36 (1H, d, *J* = 1.6 Hz), 7.41 (1H, dd, *J* = 6.7, 10.2 Hz), 8.18 (1H, s).

***N*-[(2,4-Dimethoxyphenyl)methyl]-2,5-difluoro-4-{[(1*S**,2*R**)-2-(1-methyl-1*H*-pyrazol-5-yl)cyclopentyl]oxy}-*N*-(3-methyl-1,2,4-thiadiazol-5-yl)benzene-1-sulfonamide (*rac*-5d)**

Prepared according to General Procedure B. Yield 57%. ^{1}H-NMR (500 MHz, $CDCl_3$) δ 1.74–1.99 (4H, m), 2.14–2.32 (2H, m), 2.43 (3H, s), 3.42–3.46 (1H, m), 3.69 (3H, s), 3.70 (3H, s), 3.84 (3H, s), 4.29 (1H, d, *J* = 5.9 Hz), 4.54–4.57 (1H, m), 5.24 (2H, s), 6.02 (1H, d, *J* = 2.0 Hz), 6.22 (1H, d, *J* = 2.4 Hz), 6.31 (1H, dd, *J* = 2.4, 8.3 Hz), 6.40–6.44 (1H, m), 7.15 (1H, t, *J* = 7.3 Hz), 7.38 (1H, d, *J* = 2.0 Hz), 7.50 (1H, dd, *J* = 6.8, 9.8 Hz).

***N*-[(2,4-Dimethoxyphenyl)methyl]-2,5-difluoro-4-{[(1*S**,2*R**)-2-(1-methyl-1*H*-pyrazol-5-yl)cyclopentyl]oxy}-*N*-(1,3-thiazol-2-yl)benzene-1-sulfonamide (*rac*-5e)**

Prepared according to General Procedure B. Yield 73%. ^{1}H-NMR (500 MHz, $CDCl_3$) δ 1.76‑1.83 (1H, m), 1.88‑1.98 (3H, m), 2.19‑2.25 (1H, m), 2.27‑2.33 (1H, m), 3.44‑3.49 (1H, m), 3.73 (3H, s), 3.75 (3H, s), 3.86 (3H, s), 4.61‑4.64 (1H, m), 5.18 (2H, s), 6.05 (1H, d, *J* = 2.0 Hz), 6.36‑6.38 (2H, m), 6.56 (1H, dd, *J* = 6.4, 11.2 Hz), 6.98 (1H, d, *J* = 3.4 Hz), 7.19 (1H, d, *J* = 8.3 Hz), 7.38‑7.41 (2H, m), 7.58 (1H, dd, *J* = 6.4, 10.3 Hz).

***tert*-Butyl (2,5-difluoro-4-{[(1*S**,2*R**)-2-(1-methyl-1*H*-pyrazol-5-yl)cyclohexyl]oxy}benzene-1-sulfonyl)1,3-thiazol-4-ylcarbamate (*rac*-5f)**

Prepared according to General Procedure B. Yield 57%. ^{1}H-NMR (400 MHz, $CDCl_3$) δ 1.35 (9H, s), 1.44–1.70 (4H, m), 1.88–1.91 (1H, m), 1.96–1.99 (1H, m), 2.06–2.10 (1H, m), 2.26–2.30 (1H, m), 3.00-3.06 (1H, m), 3.92 (3H, s), 4.18 (1H, dt, *J* = 3.9, 10.2 Hz), 6.04 (1H, d, *J* = 2.0 Hz), 6.57 (1H, dd, *J* = 6.3, 11.0 Hz), 7.36 (1H, d, *J* = 2.0 Hz), 7.49 (1H, d, *J* = 2.4 Hz), 7.76 (1H, dd, *J* = 6.3, 10.2 Hz), 8.78 (1H, d, *J* = 2.4 Hz).

***N*-[(2,4-Dimethoxyphenyl)methyl]-2,5-difluoro-4-{[(1*S**,2*R**)-2-(1-methyl-1*H*-pyrazol-5-yl)cyclopentyl]oxy}-*N*-(pyrimidin-4-yl)benzene-1-sulfonamide (*rac*-5g)**

Prepared according to General Procedure B. Yield 88%. ^{1}H-NMR (500 MHz, $CDCl_3$) δ 1.78–1.97 (4H, m), 2.20–2.33 (2H, m), 3.45–3.49 (1H, m), 3.77 (3H, s), 3.79 (3H, s), 3.86 (3H ,s), 4.60–4.64 (1H, m), 5.23 (2H, s), 6.05 (1H, d, *J* = 2.0 Hz), 6.40–6.42 (2H, m), 6.52 (1H, dd, *J* = 5.9, 10.7 Hz), 7.18–7.20 (2H, m), 7.40 (1H, d, *J* = 2.0 Hz), 7.76 (1H, dd, *J* = 6.4, 10.3 Hz), 8.45 (1H, d, *J* = 5.9 Hz), 8.78 (1H, s).

_N_-[(2,4-Dimethoxyphenyl)methyl]-2,5-difluoro-4-{[(1*S,2*R**)-2-(1-methyl-1*H*-pyrazol-5-yl)cyclohexyl]oxy}-*N*-(pyrimidin-4-yl)benzene-1-sulfonamide (*rac*-5h)**

Prepared according to General Procedure B. Yield 80%. ^{1}H-NMR (500 MHz, $CDCl_3$) δ 1.39‑1.68 (4H, m), 1.86‑1.96 (2H, m), 2.04‑2.07 (1H, m), 2.22–2.25 (1H, m), 2.98–3.03 (1H, m), 3.76 (3H, s), 3.77 (3H, s), 3.91 (3H ,s), 4.08–4.14 (1H, m), 5.19 (1H, d, *J* = 17.1 Hz), 5.23 (1H, d, J = 16.6 Hz), 6.02 (1H, d, *J* = 2.0 Hz), 6.39–6.40 (2H, m), 6.47 (1H, dd, *J* = 6.4, 11.2 Hz), 7.17–7.19 (2H, m), 7.33 (1H, d, *J* = 1.5 Hz), 7.67 (1H, dd, *J* = 6.4, 9.8 Hz), 8.45 (1H, d, *J* = 5.9 Hz), 8.78 (1H, s).

_N_-[(2,4-Dimethoxyphenyl)methyl]-3,5-difluoro-4-{[(1*S,2*R**)-2-(1-methyl-1*H*-pyrazol-5-yl)cyclopentyl]oxy}-*N*-(pyrimidin-4-yl)benzene-1-sulfonamide (*rac*-5i)**

Prepared according to General Procedure B. Yield 72%. ^{1}H-NMR (500 MHz, $CDCl_3$) δ 1.71–1.99 (5H, m), 2.27–2.36 (1H, m), 3.38–3.46 (1H, m), 3.65 (3H, s), 3.74 (3H, s), 3.83 (3H, s), 4.80–4.83 (1H, m), 5.13 (2H, s), 5.98 (1H, d, *J* = 1.5 Hz), 6.34 (1H, d, *J* = 2.4 Hz), 6.37 (1H, dd, *J* = 2.2, 8.5 Hz), 7.11 (1H, d, *J* = 8.3 Hz), 7.17 (1H, dd, *J* = 1.0, 5.9 Hz), 7.34 (1H, d, *J* = 2.0 Hz), 7.39 (2H, d, *J* = 7.8 Hz), 8.50 (1H, d, *J* = 5.9 Hz), 8.85 (1H, d, *J* = 1.0 Hz).

_N_-[(2,4-Dimethoxyphenyl)methyl]-2,3-difluoro-4-{[(1*S,2*R**)-2-(1-methyl-1*H*-pyrazol-5-yl)cyclopentyl]oxy}-*N*-(pyrimidin-4-yl)benzene-1-sulfonamide (*rac*-5j)**

Prepared according to General Procedure B. Yield 75%. ^{1}H-NMR (500 MHz, $CDCl_3$) δ 1.77–1.97 (4H, m), 2.22–2.34 (2H, m), 3.44–3.48 (1H, m), 3.76 (3H, s), 3.79 (3H ,s), 3.85 (3H, s), 4.72–4.75 (1H, m), 5.24 (1H, d, *J* = 17.1 Hz), 5.28 (1H, d, *J* = 16.6 Hz), 6.07 (1H, d, *J* = 2.0 Hz), 6.39–6.42 (2H, m), 6.64 (1H, t, *J* = 8.8 Hz), 7.19–7.21 (2H, m), 7.41 (1H, d, *J* = 2.0 Hz), 7.71 (1H, t, *J* = 8.8 Hz), 8.45 (1H, d, *J* = 5.9 Hz), 8.76 (1H, s).

_N_-[(2,4-Dimethoxyphenyl)methyl]-2,6-difluoro-4-{[(1_S_*,2_R_*)-2-(1-methyl-1_H_-pyrazol-5-yl)cyclopentyl]oxy}-_N_-(pyrimidin-4-yl)benzene-1-sulfonamide (*rac*-5k)

Prepared according to General Procedure B. Yield 75%. ^{1}H-NMR (500 MHz, $CDCl_3$) δ 1.72–1.95 (4H, m), 2.17–2.32 (2H, m), 3.35–3.39 (1H, m), 3.77 (3H, s), 3.82 (6H ,s), 4.62–4.65 (1H, m), 5.27 (2H, s), 6.04 (1H, d, *J* = 2.0 Hz), 6.39–6.44 (4H, m), 7.16 (1H, d, *J* = 7.3 Hz), 7.22 (1H, d, *J* = 7.3 Hz), 7.41 (1H, d, *J* = 2.0 Hz), 8.44 (1H, d, *J* = 5.9 Hz), 8.78 (1H, s).

_N_-[(2,4-Dimethoxyphenyl)methyl]-2,6-difluoro-4-{[(1_S_*,2_R_*)-2-(1-methyl-1_H_-pyrazol-5-yl)cyclohexyl]oxy}-_N_-(pyrimidin-4-yl)benzene-1-sulfonamide (*rac*-5l)

Prepared according to General Procedure B. Yield 48%. ^{1}H-NMR (500 MHz, $CDCl_3$) δ 1.38–1.67 (4H, m), 1.86–1.88 (1H, m), 1.94–1.95 (1H, m), 2.03–2.06 (1H, m), 2.22–2.24 (1H, m), 2.90–2.95 (1H, m), 3.77 (3H, s), 3.81 (3H, s), 3.86 (3H ,s), 4.10–4.15 (1H, m), 5.24 (2H, s), 5.99 (1H, d, *J* = 2.0 Hz), 6.29 (2H, d, *J* = 10.7 Hz), 6.40‑6.44 (2H, m), 7.14 (1H, dd, *J* = 1.0, 5.9 Hz), 7.21 (1H, d, *J* = 8.3 Hz), 7.34 (1H, d, *J* = 2.0 Hz), 8.44 (1H, d, *J* = 5.9 Hz), 8.78 (1H, s).

_N_-[(2,4-Dimethoxyphenyl)methyl]-2,6-difluoro-4-{[(1_S_*,2_R_*)-2-(1-methyl-1_H_-pyrazol-5-yl)cycloheptyl]oxy}-_N_-(pyrimidin-4-yl)benzene-1-sulfonamide (*rac*-5m)

Prepared according to General Procedure B. Yield 52%. ^{1}H-NMR (500 MHz, $CDCl_3$) δ 1.60‑1.98 (10H, m), 3.15 (1H, dt, *J* = 2.9, 9.3 Hz), 3.77 (3H, s), 3.81 (3H, s), 3.85 (3H ,s), 4.36–4.40 (1H, m), 5.25 (2H, s), 5.98 (1H, d, *J* = 2.0 Hz), 6.27 (2H, d, *J* = 10.7 Hz), 6.41 (1H, dd, *J* = 2.4, 8.3 Hz), 6.44 (1H, d, *J* = 2.0 Hz), 7.16 (1H, dd, *J* = 1.5, 5.9 Hz), 7.21 (1H, d, *J* = 8.3 Hz), 7.33 (1H, d, *J* = 2.0 Hz), 8.44 (1H, d, *J* = 5.9 Hz), 8.78 (1H, s).

5-Chloro-_N_-[(2,4-dimethoxyphenyl)methyl]-2-fluoro-4-{[(1_S_*,2_R_*)-2-(1-methyl-1_H_-pyrazol-5-yl)cyclopentyl]oxy}-_N_-(pyrimidin-4-yl)benzene-1-sulfonamide (*rac*-5n)

Prepared according to General Procedure B. Yield 84%. ^{1}H-NMR (500 MHz, $CDCl_3$) δ 1.73‑1.98 (4H, m), 2.17‑2.35 (2H, m), 3.48‑3.52 (1H, m), 3.76 (3H, s), 3.78 (3H, s), 3.88 (3H ,s), 4.60‑4.63 (1H, m), 5.22 (1H, d, *J* = 17.1 Hz), 5.26 (1H, d, *J* = 17.1 Hz), 6.06 (1H, d, *J* = 1.5 Hz), 6.39‑6.41 (2H, m), 6.48

(1H, d, *J* = 11.7 Hz), 7.18‑7.21 (2H, m), 7.40 (1H, s), 8.02 (1H, d, *J* = 7.3 Hz), 8.46 (1H, d, *J* = 5.9 Hz), 8.79 (1H, s).

5-Chloro-*N*-[(2,4-dimethoxyphenyl)methyl]-2-fluoro-4-{[(1*S,2*R**)-2-(1-methyl-1*H*-pyrazol-5-yl)cyclohexyl]oxy}-*N*-(pyrimidin-4-yl)benzene-1-sulfonamide (*rac*-5o)**

Prepared according to General Procedure B. Yield 86%. ^{1}H-NMR (400 MHz, $CDCl_3$) δ 1.40–1.68 (4H, m), 1.85–1.97 (2H, m), 2.04–2.10 (1H, m), 2.18–2.23 (1H, m), 3.02–3.09 (1H, m), 3.76 (3H, s), 3.76 (3H, s), 3.93 (3H, s), 4.09–4.17 (1H, m), 5.21 (2H, s), 6.03 (1H, d, *J* = 2.0 Hz), 6.38–6.45 (3H, m), 7.17–7.22 (2H, m), 7.35 (1H, d, *J* = 2.0 Hz), 7.92 (1H, d, *J* = 7.4 Hz), 8.46 (1H, d, *J* = 5.9 Hz), 8.79 (1H, d, *J* = 1.2 Hz).

5-Chloro-*N*-[(2,4-dimethoxyphenyl)methyl]-2-fluoro-4-{[(1*S*,2*R*)-2-(1-methyl-1*H*-pyrazol-5-yl)cyclohexyl]oxy}-*N*-(pyrimidin-4-yl)benzene-1-sulfonamide (5o)

Prepared according to General Procedure B. Yield 50%.

***N*-[(2,4-Dimethoxyphenyl)methyl]-2-fluoro-5-methyl-4-{[(1*S**,2*R**)-2-(1-methyl-1*H*-pyrazol-5-yl)cyclopentyl]oxy}-*N*-(pyrimidin-4-yl)benzene-1-sulfonamide (*rac*-5p)**

Prepared according to General Procedure B. Yield 50%. ^{1}H-NMR (500 MHz, $CDCl_3$) δ 1.74‑1.95 (4H, m), 2.16–2.34 (2H, m), 2.20 (3H, s), 3.41 (1H, dt, *J* = 4.9, 8.3 Hz), 3.76 (3H, s), 3.80 (3H, s), 3.84 (3H ,s), 4.62‑4.65 (1H, m), 5.26 (2H, s), 6.04 (1H, d, *J* = 2.0 Hz), 6.37‑6.42 (3H, m), 7.20 (1H, d, *J* = 8.3 Hz), 7.26-7.28 (1H, m), 7.40 (1H, d, *J* = 1.5 Hz), 7.76 (1H, d, *J* = 7.8 Hz), 8.42 (1H, d, *J* = 5.9 Hz), 8.76 (1H, s).

***N*-[(2,4-Dimethoxyphenyl)methyl]-2-fluoro-5-methyl-4-{[(1*S**,2*R**)-2-(1-methyl-1*H*-pyrazol-5-yl)cyclohexyl]oxy}-*N*-(pyrimidin-4-yl)benzene-1-sulfonamide (*rac*-5q)**

Prepared according to General Procedure B. Yield 42%. ^{1}H-NMR (500 MHz, $CDCl_3$) δ 1.40‑1.64 (4H, m), 1.86–1.88 (1H, m), 1.92–1.93 (1H, m), 2.02–2.06 (1H, m), 2.02 (3H, s), 2.23–2.26 (1H, m), 2.97–3.02 (1H, m), 3.76 (3H, s), 3.78 (3H, s), 3.89 (3H ,s), 4.01–4.14 (1H, m), 5.24 (2H, s), 5.98 (1H, d, *J* = 2.0 Hz), 6.36-6.40 (3H, m), 7.19 (1H, d, *J* = 8.8 Hz), 7.28 (1H, dd, *J* = 1.5, 5.9 Hz), 7.35 (1H, d, *J* = 2.0 Hz), 7.66 (1H, d, *J* = 7.8 Hz), 8.43 (1H, d, *J* = 5.9 Hz), 8.77 (1H, d, *J* = 1.0 Hz).

2,5-Difluoro-4-[2-(1-methyl-1*H*-pyrazol-5-yl)ethoxy]-*N*-(1,2,4-thiadiazol-5-yl)benzene-1-sulfonamide (6a)

Prepared according to General Procedure C. Yield 19%. ^{1}H-NMR (400 MHz, $CDCl_3$) δ 3.17 (2H, t, *J* = 6.3 Hz), 3.88 (3H, s), 4.23 (2H, t, *J* = 6.3 Hz), 6.11 (1H, d, *J* = 1.6 Hz), 6.69 (1H, dd, *J* = 6.3, 10.9 Hz), 7.41 (1H, d, *J* = 2.0 Hz), 7.65 (1H, dd, *J* = 6.6, 9.8 Hz), 8.06 (1H, s); Anal. calculated for $C_{14}H_{13}F_2N_5O_3S_2$•1.1H_2O: C, 39.92; H, 3.64; N, 16.63. Found C, 40.10; H, 3.45; N, 16.37; MS(ESI) *m/z*: 402$[M+H]^+$.

2,5-Difluoro-4-{[(1*S,2*R**)-2-(1-methyl-1*H*-pyrazol-5-yl)cyclopentyl]oxy}-*N*-(1,2,4-thiadiazol-5-yl)benzene-1-sulfonamide (*rac*-6b)**

Prepared according to General Procedure C. Yield 83%. ^{1}H-NMR (400 MHz, $CDCl_3$) δ 1.76–2.00 (4H, m), 2.18–2.35 (2H, m), 3.34–3.50 (1H, m), 3.87 (3H, s), 4.60–4.64 (1H, m), 6.07 (1H, d, *J* = 1.6 Hz), 6.59 (1H, dd, *J* = 6.3, 11.0 Hz), 7.43 (1H, d, *J* = 2.0 Hz), 7.66 (1H, dd, *J* = 6.7, 9.8 Hz), 8.07 (1H, s); HRMS (ESI) *m/z*: $[M + H]^+$ calculated for $C_{17}H_{18}F_2N_5O_3S$, 442.0813; found 442.0809.

2,5-Ddifluoro-4-{[(1*S,2*R**)-2-(1-methyl-1*H*-pyrazol-5-yl)cyclohexyl]oxy}-*N*-(1,2,4-thiadiazol-5-yl)benzene-1-sulfonamide (*rac*-6c)**

Prepared according to General Procedure C. Yield 43%. ^{1}H-NMR (400 MHz, DMSO-d_6) δ 1.37–1.60 (4H, m), 1.71–1.81 (2H, m), 1.90–1.94 (1H, m), 2.16–2.19 (1H, m), 3.07–3.13 (1H, m), 3.79 (3H, s), 4.57 (1H, dt, *J* = 4.3, 9.8 Hz), 6.09 (1H, d, *J* = 2.0 Hz), 7.22 (1H, d, *J* = 2.0 Hz), 7.34 (1H, dd, *J* = 6.7, 11.7 Hz), 7.54 (1H, dd, *J* = 6.7, 10.6 Hz), 8.53 (1H, s); MS(FAB) *m/z*: 456$[M+H]^+$.

2,5-Difluoro-4-{[(1*S,2*R**)-2-(1-methyl-1*H*-pyrazol-5-yl)cyclopentyl]oxy}-*N*-(3-methyl-1,2,4-thiadiazol-5-yl)benzene-1-sulfonamide (*rac*-6d)**

Prepared according to General Procedure C. Yield 80%. ^{1}H-NMR (400 MHz, $CDCl_3$) δ 1.73–1.96 (4H, m), 2.16–2.30 (2H, m), 2.49 (3H, s), 3.40–3.46 (1H, m), 3.84 (3H, s), 4.56–4.60 (1H, m), 6.04 (1H, d, *J* = 1.6 Hz), 6.54 (1H, dd, *J* = 6.5, 11.1 Hz), 7.40 (1H, d, *J* = 1.6 Hz), 7.61 (1H, dd, *J* = 6.6, 9.8 Hz); HRMS (ESI) *m/z*: $[M + H]^+$ calculated for $C_{18}H_{20}F_2N_5O_3S$, 456.0970; found 456.0982.

2,5-Difluoro-4-{[(1*S,2*R**)-2-(1-methyl-1*H*-pyrazol-5-yl)cyclopentyl]oxy}-*N*-(1,3-thiazol-2-yl)benzene-1-sulfonamide (*rac*-6e)**

Prepared according to General Procedure C. Yield 82%. ^{1}H-NMR (500 MHz, $CDCl_3$) δ 1.77–1.96 (4H, m), 2.19–2.23 (1H, m), 2.27–2.32 (1H, m), 3.44–3.48 (1H, m), 3.86 (3H, s), 4.59–4.62 (1H, m), 6.05 (1H, s), 6.54–6.57 (2H, m), 7.17 (1H, d, *J* = 4.4 Hz), 7.40 (1H, s), 7.71 (1H, dd, *J* = 6.4, 9.8 Hz); HRMS (ESI) *m/z*: $[M + H]^+$ calculated for $C_{18}H_{19}F_2N_4O_3S_2$, 441.0788; found 441.0861.

2,5-Difluoro-4-{[(1*S,2*R**)-2-(1-methyl-1*H*-pyrazol-5-yl)cyclohexyl]oxy}-*N*-(1,3-thiazol-4-yl)benzene-1-sulfonamide (*rac*-6f)**

The solution of *tert*-butyl (2,5-difluoro-4-{[(1*S*,2*R*)-2-(1-methyl-1*H*-pyrazol-5-yl)cyclohexyl]oxy}benzene-1-sulfonyl)1,3-thiazol-4-ylcarbamate (177 mg, 0.319 mmol) and TFA (1.0 mL) in CH_2Cl_2 (1.0 mL) was stirred at room temperature for 16 h. The reaction mixture was concentrated, and the residue was purified with silica gel chromatography to yield the title compound (260 mg, 87%) as a colorless solid. ^{1}H-NMR (400 MHz, $CDCl_3$) δ 1.40–1.69 (4H, m), 1.85–1.88 (1H, m), 1.92–1.95 (1H, m), 2.03–2.07 (1H, m), 2.21–2.25 (1H, m), 2.95–3.01 (1H, m), 3.89 (3H, s), 4.09 (1H, dt, *J* = 3.9, 10.6 Hz), 6.01 (1H, d, *J* = 2.0 Hz), 6.48 (1H, dd, *J* = 6.3, 11.0 Hz), 6.89 (1H, d, *J* = 2.4 Hz), 7.33 (1H, d, *J* = 1.6 Hz), 7.51 (1H, dd, *J* = 7.0, 10.2 Hz), 8.72 (1H, d, *J* = 2.4 Hz); HRMS (ESI) *m/z*: $[M + H]^+$ calculated for $C_{19}H_{21}F_2N_4O_3S_2$, 455.1018; found 455.1028.

2,5-Difluoro-4-{[(1*S,2*R**)-2-(1-methyl-1*H*-pyrazol-5-yl)cyclopentyl]oxy}-*N*-(pyrimidin-4-yl)benzene-1-sulfonamide (*rac*-6g)**

Prepared according to General Procedure C. Yield 99%. ^{1}H-NMR (500 MHz, DMSO-d_6) δ 1.66‑1.83 (4H, m), 2.19–2.27 (2H, m), 3.47–3.51 (1H, m), 3.76 (3H ,s), 4.92–4.95 (1H, m), 6.17 (1H, s), 6.97 (1H, br), 7.20–7.24 (1H, m), 7.30 (1H, s), 7.68–7.71 (1H, m), 8.25 (1H, br), 8.57 (1H, s). Anal. calculated for $C_{19}H_{19}F_2N_5O_3S$: C, 52.41; H, 4.40; N, 16.08. Found C, 52.12; H, 4.23; N, 16.05; MS(ESI) *m/z*: 436[M+H]+.

2,5-Difluoro-4-{[(1*S,2*R**)-2-(1-methyl-1*H*-pyrazol-5-yl)cyclohexyl]oxy}-*N*-(pyrimidin-4-yl)benzene-1-sulfonamide (*rac*-6h)**

Prepared according to General Procedure C. Yield 65%. ^{1}H-NMR (500 MHz, $CDCl_3$) δ 1.38–1.68 (4H, m), 1.86–1.89 (1H, m), 1.93–1.95 (1H, m), 2.05–2.07 (1H, m), 2.22‑2.25 (1H, m), 2.97‑3.02 (1H, m), 3.90 (3H, s), 4.07–4.12 (1H, m), 6.02 (1H, d, *J* = 2.0 Hz), 6.50 (1H, dd, *J* = 6.4, 11.2 Hz), 7.24 (1H, d, *J* = 6.4 Hz), 7.33 (1H, d, *J* = 2.0 Hz), 7.66 (1H, dd, *J* = 6.8, 10.3 Hz), 8.38 (1H, d, *J* = 6.4 Hz), 8.80 (1H, s); HRMS (ESI) *m/z*: $[M + H]^+$ calculated for $C_{20}H_{22}F_2N_5O_3S$, 450.1406; found 450.1420. Anal. calculated for $C_{20}H_{21}F_2N_5O_3S$: C, 53.44; H, 4.71; N, 15.58. Found C, 53.10; H, 4.57; N, 15.34.

3,5-Difluoro-4-{[(1*S,2*R**)-2-(1-methyl-1*H*-pyrazol-5-yl)cyclopentyl]oxy}-*N*-(pyrimidin-4-yl)benzene-1-sulfonamide (*rac*-6i)**

Prepared according to General Procedure C. Yield 53%. ^{1}H-NMR (500 MHz, $CDCl_3$) δ 1.70–2.02 (5H, m), 2.29–2.35 (1H, m), 3.40–3.44 (1H, m), 3.82 (3H, s), 4.80–4.84 (1H, m), 5.97 (1H, s), 7.15 (1H, d, *J* = 5.9 Hz), 7.33 (1H, s), 7.49 (2H, d, *J* = 6.3 Hz), 8.37 (1H, s), 8.71 (1H, s). Anal. calculated for $C_{19}H_{19}F_2N_5O_3S•0.40H_2O$: C, 51.55; H, 4.51; N, 15.82. Found C, 51.34; H, 4.18; N, 15.70; MS(ESI) *m/z*: 436$[M+H]^+$.

2,3-Difluoro-4-{[(1*S,2*R**)-2-(1-methyl-1*H*-pyrazol-5-yl)cyclopentyl]oxy}-*N*-(pyrimidin-4-yl)benzene-1-sulfonamide (*rac*-6j)**

Prepared according to General Procedure C. Yield 41%. ^{1}H-NMR (500 MHz, $CDCl_3$) δ 1.77‑1.96 (4H, m), 2.20–2.34 (2H, m), 3.44–3.48 (1H, m), 3.84 (3H ,s), 4.71–4.74 (1H, m), 6.06 (1H, d, *J* = 1.5 Hz), 6.66 (1H, t, *J* = 7.8 Hz), 7.24–7.25 (1H, m), 7.41 (1H, s), 7.70 (1H, t, *J* = 9.3 Hz), 8.37 (1H, d, *J* = 6.4 Hz), 8.81 (1H, s); HRMS (ESI) *m/z*: $[M + H]^+$ calculated for $C_{19}H_{20}F_2N_5O_3S$, 436.1249; found 436.1273.

2,6-Difluoro-4-{[(1*S,2*R**)-2-(1-methyl-1*H*-pyrazol-5-yl)cyclopentyl]oxy}-*N*-(pyrimidin-4-yl)benzene-1-sulfonamide (*rac*-6k)**

Prepared according to General Procedure C. Yield 74%. ^{1}H-NMR (500 MHz, $CDCl_3$) δ 1.72–1.95 (4H, m), 2.17–2.31 (2H, m), 3.35–3.39 (1H, m), 3.82 (3H ,s), 4.61–4.64 (1H, m), 6.04 (1H, d, *J* = 2.0 Hz), 6.41 (2H, d, *J* = 10.7 Hz), 7.40–7.42 (2H, m), 8.42 (1H, d, *J* = 5.9 Hz), 8.87 (1H, s). Anal. calculated for $C_{19}H_{19}F_2N_5O_3S•0.50H_2O$: C, 51.35; H, 4.54; N, 15.76. Found C, 51.61; H, 4.37; N, 15.43; MS(ESI) *m/z*: 436[M+H]+.

2,6-Difluoro-4-{[(1*S,2*R**)-2-(1-methyl-1*H*-pyrazol-5-yl)cyclohexyl]oxy}-*N*-(pyrimidin-4-yl)benzene-1-sulfonamide (*rac*-6l)**

Prepared according to General Procedure C. Yield 30%. ^{1}H-NMR (400 MHz, $CDCl_3$) δ 1.38‑1.65 (4H, m), 1.85–1.88 (1H, m), 1.93–1.95 (1H, m), 2.03–2.08 (1H, m), 2.22–2.24 (1H, m), 2.89–2.96 (1H, m), 3.86 (3H, s), 4.09–4.15 (1H, m), 6.00 (1H, d, J = 2.0 Hz), 6.32 (2H, d, J = 10.6 Hz), 7.34 (1H, d, J = 2.0 Hz), 7.41 (1H, d, J = 6.7 Hz), 8.41 (1H, d, J = 6.3 Hz), 8.80 (1H, s); HRMS (ESI) *m/z*: $[M + H]^+$ calculated for $C_{20}H_{22}F_2N_5O_3S$, 450.1406; found 450.1422. Anal. calculated for $C_{20}H_{21}F_2N_5O_3S•0.40H_2O$: C, 52.60; H, 4.81; N, 15.34. Found C, 52.64; H, 4.73; N, 15.03.

2,6-Difluoro-4-{[(1*S,2*R**)-2-(1-methyl-1*H*-pyrazol-5-yl)cycloheptyl]oxy}-*N*-(pyrimidin-4-yl)benzene-1-sulfonamide (*rac*-6m)**

Prepared according to General Procedure C. Yield 40%. ^{1}H-NMR (500 MHz, DMSO-d_6) δ 1.52–1.92 (10H, m), 3.18–3.21 (1H, m), 3.76 (3H, s), 4.73–4.77 (1H, m), 6.10 (1H, d, J = 2.0 Hz), 6.72 (2H, d, J = 11.2 Hz), 6.94 (1H, br), 7.19 (1H, d, J = 1.5 Hz), 8.29 (1H, br), 8.58 (1H, s); HRMS (ESI) *m/z*: $[M + H]^+$ calculated for $C_{21}H_{24}F_2N_5O_3S$, 464.1562; found 464.1566. Anal. calculated for $C_{21}H_{23}F_2N_5O_3S•0.80H_2O$: C, 52.78; H, 5.19; N, 14.65. Found C, 52.82; H, 5.04; N, 14.44.

5-Chloro-2-fluoro-4-{[(1*S,2*R**)-2-(1-methyl-1*H*-pyrazol-5-yl)cyclopentyl]oxy}-*N*-(pyrimidin-4-yl)benzene-1-sulfonamide (*rac*-6n)**

Prepared according to General Procedure C. Yield 51%. ^{1}H-NMR (500 MHz, $CDCl_3$) δ 1.79–1.96 (4H, m), 2.20–2.33 (2H, m), 3.48–3.52 (1H, m), 3.89 (3H ,s), 4.60–4.63 (1H, m), 6.05 (1H, s), 6.54 (1H, d, J = 11.7 Hz), 7.26–7.27 (1H, m), 7.39 (1H, s), 8.02 (1H, d, J = 7.3 Hz), 8.39 (1H, J = 4.9 Hz), 8.81 (1H, s); HRMS (ESI) *m/z*: $[M + H]^+$ calculated for $C_{19}H_{20}ClFN_5O_3S$, 452.0954; found 452.0951. Anal. calculated for $C_{19}H_{19}ClFN_5O_3S•0.60H_2O$: C, 49.32; H, 4.40; N, 15.14. Found C, 49.24; H, 4.13; N, 15.05.

5-Chloro-2-fluoro-4-{[(1*S,2*R**)-2-(1-methyl-1*H*-pyrazol-5-yl)cyclohexyl]oxy}-*N*-(pyrimidin-4-yl)benzene-1-sulfonamide (*rac*-6o)**

Prepared according to General Procedure C. Yield 72%. ^{1}H-NMR (400 MHz, $CDCl_3$) δ 1.36–1.70 (4H, m), 1.85–1.96 (2H, m), 2.03–2.11 (1H, m), 2.18–2.23 (1H, m), 3.01–3.09 (1H, m), 3.93 (3H, s), 4.09–

4.17 (1H, m), 6.03 (1H, d, *J* = 2.0 Hz), 6.47 (1H, d, *J* = 11.7 Hz), 7.23–7.27 (1H, m), 7.34 (1H, d, *J* = 2.0 Hz), 7.94 (1H, d, *J* = 7.8 Hz), 8.39 (1H, d, *J* = 6.3 Hz), 8.81 (1H, s); HRMS (ESI) *m/z*: $[M + H]^+$ calculated for $C_{20}H_{22}ClFN_5O_3S$, 466.1110; found 466.1135. Anal. calculated for $C_{20}H_{21}ClFN_5O_3S \bullet 1.0H_2O$: C, 49.64; H, 4.79; N, 14.47. Found C, 49.99; H, 4.45; N, 14.18.

5-Chloro-2-fluoro-4-{[(1*S*,2*R*)-2-(1-methyl-1*H*-pyrazol-5-yl)cyclohexyl]oxy}-*N*-(pyrimidin-4-yl)benzene-1-sulfonamide (6o, DS-1971a)

Prepared according to General Procedure C. Yield 99%. HRMS (ESI) *m/z*: $[M + H]^+$ calculated for $C_{20}H_{22}ClFN_5O_3S$, 466.1110; found 466.1131. Anal. calculated for $C_{20}H_{21}ClFN_5O_3S$: C, 51.55; H, 4.54; N, 15.03. Found C, 51.49; H, 4.58; N, 14.97; $[\alpha]^{25}_D = +2.28$ (*c* 1.05, DMSO).

2-Fluoro-5-methyl-4-{[(1*S,2*R**)-2-(1-methyl-1*H*-pyrazol-5-yl)cyclopentyl]oxy}-*N*-(pyrimidin-4-yl)benzene-1-sulfonamide (*rac*-6p)**

Prepared according to General Procedure C. Yield 98%. ^{1}H-NMR (500 MHz, $CDCl_3$) δ 1.73–1.93 (4H, m), 2.18–2.34 (2H, m), 2.21 (3H, s), 3.41 (1H, dt, *J* = 4.4, 7.8 Hz), 3.84 (3H ,s), 4.62–4.65 (1H, m), 6.04 (1H, d, *J* = 1.5 Hz), 6.44 (1H, d, *J* = 11.7 Hz), 7.24–7.25 (1H, m), 7.39 (1H, d, *J* = 2.0 Hz), 7.75 (1H, d, *J* = 7.8 Hz), 8.41 (1H, d, *J* = 5.9 Hz), 8.86 (1H, br); HRMS (ESI) *m/z*: $[M + H]^+$ calculated for $C_{20}H_{23}FN_5O_3S$, 432.1427; found 432.1517. Anal. calculated for $C_{20}H_{22}FN_5O_3S$: C, 55.67; H, 5.14; N, 16.23. Found C, 55.30; H, 5.11; N, 16.08; MS(ESI) *m/z*: $432[M+H]^+$.

2-Fluoro-5-methyl-4-{[(1*S,2*R**)-2-(1-methyl-1*H*-pyrazol-5-yl)cyclohexyl]oxy}-*N*-(pyrimidin-4-yl)benzene-1-sulfonamide (*rac*-6q)**

Prepared according to General Procedure C. Yield 99%. ^{1}H-NMR (500 MHz, $CDCl_3$) δ 1.40–1.60 (4H, m), 1.85–1.87 (1H, m), 1.91–1.92 (1H, m), 2.04–2.06 (1H, m), 2.05 (3H, s), 2.23–2.25 (1H, m), 2.96–3.02 (1H, m), 3.88 (3H ,s), 4.10–4.14 (1H, m), 5.98 (1H, d, *J* = 2.0 Hz), 6.42 (1H, d, *J* = 12.2 Hz), 7.23 (1H, d, *J* = 5.4 Hz), 7.34 (1H, d, *J* = 1.5 Hz), 7.67 (1H, d, *J* = 8.3 Hz), 8.40 (1H, d, *J* = 6.4 Hz), 8.86 (1H, br); HRMS (ESI) *m/z*: $[M + H]^+$ calculated for $C_{21}H_{25}FN_5O_3S$, 446.1657; found 466.1673. Anal. calculated for $C_{21}H_{24}FN_5O_3S \bullet 0.50H_2O$: C, 55.49; H, 5.54; N, 15.41. Found C, 55.51; H, 5.43; N, 15.20; MS(ESI) *m/z*: $446[M+H]^+$.

High-Throughput Electrophysiological Evaluation

The IonWorks Quattro system (version 2.0, serial number Q0047, Molecular Devices) was used for electrophysiological recordings. A cell suspension containing 2×10^6 cells/mL was prepared in the reservoir. A 384-well plate containing the test compounds (three-fold higher than the final test concentration) was placed in the plate-1 position. A PatchPlate was clamped into the PatchPlate station. Once the experiment began, 3.5 μL of Dulbecco's phosphate-buffered saline (DPBS, with calcium and magnesium, Sigma-Aldrich Co. LLC.) was added to each well of the PatchPlate by the fluidics-head (F-head), and its underside was perfused with internal solution with the following composition: 100.0 mM potassium D-gluconate, 40.0 mM KCl, 3.2 mM $MgCl_2$, 5.0 EGTA, and 5.0 HEPES (pH 7.27 using 1 M KOH). After priming and debubbling, the electronics-head (E-head) moved around the PatchPlate to perform a whole test. The F-head then dispensed 3.5 μL of the cell suspension ($hNa_V1.1/\beta1/\beta2$/HEK293A, $hNa_V1.5/\beta1/\beta2$/HEK293A, $hNa_V1.7/\beta1/\beta2$/HEK293A, or $mNa_V1.7/\beta1/\beta2$/HEK293A) into each well of the PatchPlate, and the cells were given 400 s to reach and seal the hole in the well. Then, the E-head moved around the PatchPlate to determine the seal resistance in each well. Next, the solution on the underside of the PatchPlate was changed, to solution with the following composition: 100.0 mM potassium D-gluconate, 40.0 mM KCl, 3.2 mM $MgCl_2$, 5.0 EGTA, 5.0 HEPES (pH 7.27 using 1 M KOH), plus 100 μg/mL of amphotericin B (lot number 071M4069V, Sigma-Aldrich Co. LLC.). Patch perforation proceeded for 10 min, after which the E-head moved around the PatchPlate to measure the Na_V current.

After these pre-compound measurements, the F-head added 3.5 μL of solution from each well of the compound plate to each well of the PatchPlate. After approximately 5.5 min of incubation, the E-head moved around the PatchPlate to measure post-compound Na_V currents. Experiments were performed at room temperature.

The pre- and post-compound Na_V current amplitudes were measured from the peak current response by subtracting the baseline current (the average current amplitude between 44 and 49 ms of the test pulse period). The raw data were processed as follows using Microsoft Excel 2010 (Microsoft Corporation). If

seal resistance was poor (< 20 MΩ), the difference in the offset/intercept value between the pre- and post-compound measurements was large (>5 mV), or the pre-compound Na_V current amplitude was smaller than one-third of the average of the whole pre-compound Na_V current amplitude, the data were eliminated. The degree of Na_V current block was corrected by vehicle control currents as follows:

% inhibition = 100 × (1 − relative current [compound]/mean relative current [vehicle])

where relative current (compound) is the value of the post-compound Na_V current amplitude divided by the respective pre-compound Na_V current amplitude, and mean relative current (vehicle) is the mean value of the post-vehicle Na_V current amplitude divided by the pre-vehicle Na_V current amplitude.

If the compound inhibited the Na_V current by more than 50%, a concentration-response curve was obtained. Data were fitted with a four-parameter logistic equation:

$$Y = \text{Bottom} + (\text{Top} - \text{Bottom})/(1 + 10^{[(\text{LogIC50} - X) \times \text{HillSlope}]})$$

where, X is the drug concentration logarithm, Y is the % inhibition, and HillSlope is the Hill coefficient. The IC_{50} was calculated using GraphPad Prism 4.03 (GraphPad Software, Inc.). The voltage program for each Na_V subtype or species is summarized in Table 9.

Table 9. Voltage Program.

	$hNa_V1.1$	$hNa_V1.5$	$hNa_V1.7$	$mNa_V1.7$
Holding pulse (for 5 s)	−100 mV	−120 mV	−100 mV	−100 mV
Test pulse (for analysis of resting-state channels, for 50 ms)	0 mV	−20 mV	−10 mV	−10 mV
Repolarizing pulse (for 200 ms)	−100 mV	−120 mV	−100 mV	−100 mV
Second conditioning pulse (for 2 s)	−43 mV	−68 mV	−59 mV	−56 mV
Test pulse (for analysis of inactivated-state channels, for 50 ms)	0 mV	−20 mV	−10 mV	−10 mV

Log D, PAMPA, Solubility, Microsomal Stability, and Protein Binding Assay

Each assay was performed as previously described.[27,28,29]

MBI Assay[30]

MBI inactivation against CYP3A4 was estimated as the percentage of enzymatic activity (1'-hydroxylation of midazolam) remaining after preincubation of test compounds for 30 min in pooled HLM.

GSH-trapping assay[31]

For the GSH-trapping experiments, each test compound (500 μM) was incubated with HLM (2 mg of protein/mL) supplemented with an NADPH-generating system and an equimolar mixture of GSH and stable isotope-labeled GSH ([$^{13}C_2$, ^{15}N-Gly]GSH). After 60-minutes incubation, the reaction was terminated with MeCN containing *n*-PrOH, followed by centrifugation and concentration of the supernatant. Incubation without NADP or a substrate was performed to obtain control samples. The analytical samples were subjected to LC-MS/MS analysis in full-scan MSE mode using a Q-Tof Xevo mass spectrometer (Waters).

Effects of DS-1971a on Peak Currents of Voltage-Gated Sodium Channels Na_V1.1/1.2/1.3/1.4/1.5/1.6/1.7/1.8 (Whole Cell Manual Patch Clamp Method)

The 35 mm culture dishes, upon which cells were seeded at a density that allowed single cells to be recorded, were placed on the dish holder of the microscope and continuously perfused (at approximately 1 mL/min). All solutions applied to cells, including the pipette solution, were maintained at room temperature. After a Gigaohm seal was formed between the patch electrodes and individual voltage-gated sodium channel-transfected cells (pipette resistance range: 4.0 MΩ - 5.0 MΩ; seal resistance range: > 1 GΩ), cell membranes across the pipette tip were ruptured to assure electrical access to the cell interior (whole cell patch configuration). After whole-cell access was obtained, series resistance and leakage currents were monitored for 3–5 min. Uncompensated series resistance should be < 10 MΩ (< 12.5 MΩ

in case of ND7/23 hNa$_V$1.8), and leakage current should be < 5% (< 10% in case of ND7/23 hNa$_V$1.8) at the holding potential (-50 mV) of the peak current amplitude.

Once a stable whole-cell patch configuration was established, sodium inward currents were measured upon depolarization of the cell membrane to the activation potential, as indicated in Table 10, for 10 ms (15 ms in case of DMSO and test item of ND7/23 hNa$_V$1.8) from a holding potential (Table 10) until the current amplitude was stabilized. After stabilization of the current response, cells were pulsed continuously by the following voltage protocol: the membrane potential was pulsed to the holding potential (Table 10) for 1 s (to reprime channels not bound by drug) from the holding potential of −50 mV, and then given a 10 ms (15 ms in case of DMSO and test item ND7/23 hNa$_V$1.8) test pulse to the activation potential (Table 10) to elicit current. This voltage protocol was run with an interval of 9 s until currents were stabilized.

Once control recordings were obtained, recordings to determine the compound blockage began. Cells were pulsed by the voltage protocol indicated above for at least 1 min perfused with bath solution to confirm the current stabilization. Subsequently, perfusion of bath solution containing the test compound began. During wash-in of the test item, the reference compound or vehicle for the same voltage protocol indicated above, was run continuously at 9 s intervals for 10 min after the start of the analysis.

Table 10. Cell lines and Voltages Used to Stimulate Na$_V$s.

Ion channel target	Cell line	Holding potential	Activation potential
hNa$_V$1.1	CHO hNa$_V$1.1	−120 mV	0 mV
mNa$_V$1.1	HEK293A mNa$_V$1.1/β1/β2	−120 mV	0 mV
hNa$_V$1.2	CHO hNa$_V$1.2	−120 mV	0 mV
hNa$_V$1.3	CHO hNa$_V$1.3	−120 mV	0 mV
hNa$_V$1.4	HEK293A hNa$_V$1.4/β1/β2	−120 mV	0 mV
hNa$_V$1.5	CHO hNa$_V$1.5	−140 mV	−20 mV

$mNa_V1.5$	HEK293A $mNa_V1.5/\beta1/\beta2$	−140 mV	−20 mV
$hNa_V1.6$	CHO $hNa_V1.6$	−120 mV	0 mV
$hNa_V1.7$	CHO $hNa_V1.7$	−120 mV	−10 mV
$mNa_V1.7$	HEK293A $mNa_V1.7/\beta1/\beta2$	−120 mV	−10 mV
$hNa_V1.8$	ND7/23 $hNa_V1.8$	−120 mV	0 mV

Effects of DS-1971a on Peak Tail Current of hERG (Whole Cell Manual Patch Clamp Method)

hERG-transfected human embryo kidney 293 (HEK293) cells were perfused with 10, 30, and 100 μmol/L DS-1971a. Cells were perfused (perfusion speed: approximately 4 mL/min) with the external solution (contents: NaCl, 137; KCl, 4; HEPES, 10; $CaCl_2$, 1.8; $MgCl_2$, 1; glucose, 10 mmol/L; adjusted to pH 7.32 and 7.37 with NaOH) in a bath chamber. Glass pipettes filled with the internal solution (contents: KCl, 130; $MgCl_2$, 1; EGTA, 5; HEPES, 10; ATP, 5 mmol/L; adjusted to pH 7.21 with KOH) with a resistance of 2.1 to 3.6 MΩ were used to record the hERG current. The cell membrane voltage was held at -80 mV via a patch clamp amplifier (EPC8, HEKA) using patch clamp software (Clampex 9.0 [pCLAMP 9], Axon Instruments, Molecular Devices). The test pulse was applied as follows: step from −80 mV to +20 mV for 1.5 s, step to -40 mV for 1.5 s, then step to a holding potential of −80 mV. This voltage protocol was applied continuously to cells once every 15 s. After the peak current for each voltage protocol was stable at 500 pA or higher for at least 1 min, the cell was perfused with the external solution containing the test article. In the kinetics assay, the voltage pulses were run continuously for 20 min (10 min for perfusion of the test article, and 10 min following the washout).

Effect on Mechanical Hypersensitivity

The analgesic effects of DS-1971a were investigated in models of SNL[24] and PSL[21], using male Slc:ddY mice, which were prepared as previously described. Two-weeks after model preparation, the animals were administered the test article or the vehicle orally, and the mechanical pain threshold in the hind paw was measured using an electronic von Frey anesthesiometer (Dynamic Plantar Aesthesiometer, model 37400;

Ugo Basile, Varese, Italy). Mechanical stimulation was applied to the left hind paw in a stepwise manner (from 0 to 30 g in 40 s at 0.5 g/step). The maximal cut-off was set as 30 g to prevent tissue damage. No animal reached the cut-off value.

Effect on Thermal Hyperalgesia

The analgesic effects of DS-1971a were evaluated in PSL model mice. Male Slc:ddY mice were used, and the PSL model was prepared as previously described.[21] After the development of hyperalgesia, animals were administered the test article or vehicle orally, and the thermal pain threshold in the hind paw was measured using a paw thermal stimulator (Plantar Test 7370, Ugo Basile, Varese, Italy, or UCSD, San Diego, CA, USA). A 20 s cut-off time was employed to avoid tissue damage. No animal reached the cut-off value. The rate of improvement (%) was calculated according to the following formula, and the half maximal effective dose (ED_{50}) was determined.

Improvement rate (%) = [(Pain threshold in DS-1971a group − Mean pain threshold in the model control group)/(Mean pain threshold in the normal control group − Mean pain threshold in the model control group)] × 100.

Pharmacokinetic (PK) Study

Exposure of the test compound in animals was determined by collecting blood samples at several time points post-dose. The plasma was separated from the blood by centrifugation, and stored at −70°C until use in subsequent analyses. The plasma concentration of the compound was determined by the LC-MS/MS method using API 4000 (Applied Biosystems/MDS SCIEX). PK parameters were calculated via non-compartmental analysis. Animals and formulations used in the PK studies are summarized in Table 11.

Table 11. Animals and Formulations used in PK studies

Species	Strain	Sex	Formulation (oral)	Formulation (intravenous)
Monkey	Cynomolgus	Male	10% DMA in saline	10% DMA in saline
Dog	Beagle	Male	0.5% MC	10% DMA in saline
Rat	SD	Male	10% DMA in saline	10% DMA in saline
Mouse	ddY	Male	10% DMA in saline	10% DMA in saline

CNS Safety Pharmacology Study in Mice (Irwin's Multiple Observation)

Male Crl:CD1(ICR) mice (*n* = 6/group; 7-weeks-old) were treated once with DS-1971a at 0, 100, 300, and 1000 mg/kg. The general physical condition and behavior of animals were observed 0, 0.5, 2, 6, and 24 h after administration, following a modified Irwin's multiple observation method.[32]

CNS Safety Pharmacology Study in Mice (Locomotor Activity)

Male Crl:CD1(ICR) mice (*n* = 8/group; 7 weeks old) were treated once with DS-1971a at dose levels of 0, 100, 300, and 1000 mg/kg. Following administration of vehicle or test article, animals were housed in a polycarbonate cage lined with bedding under a wire-mesh floor. Measurements began immediately after the animals were placed in the cages. Spontaneous locomotor activity was measured for every 10 min, from 2 until 3 h following administration using Supermex (SM-32, Muromachi Kikai Co., Ltd.).

CNS Safety Pharmacology Study in Mice (Motor Coordination)

Male Crl:CD1(ICR) mice (*n* = 8/group; 7-weeks-old) were treated once with DS-1971a at 0, 100, 300, and 1000 mg/kg. The animals were trained in advance on the rotating spindle of the rota-rod (MK-600, Muromachi Kikai Co., Ltd.) at 6 rpm to acclimate. Before administration, the animals were placed on the spindle of the rota-rod, and were then allowed to walked for 3 min; one of three performances was used for the experiment. After administration, the animals were placed on the spindle of the rota-rod, rotating at 6 rpm, and allowed to walk for 1 min. Measurements were made for each animal, as all animals walked through 1 min in the first trial. Motor coordination was measured 0, 0.5, and 2 h after administration.

Respiratory Safety Pharmacology Study in Mice

Male Crl:CD1(ICR) mice (*n* = 8/group; 7-weeks-old) were treated once with DS-1971a at 0, 100, 300, and 1000 mg/kg. Prior to the pre-administration measurement, each animal was placed in a chamber for 6 min for acclimation. Respiratory function was measured with a WBP system (BioSystem XA for Windows, ver. 2.10.5; Buxco Electronics, Inc.). Respiratory rate (RR), tidal volume (TV), and min volume (MV) were measured 1 and 2 h before administration and at 0.5, 2, 6, and 24 h after administration. Respiratory functions were recorded on a computer for at least 6 min starting immediately after the animals were placed in the chambers.

Cardiovascular Safety Pharmacology Study in Cynomolgus Monkeys

Conscious, unrestrained male cynomolgus monkeys (n = 4; 5-years-old) were treated once with DS-1971a at escalating doses of 0, 30, 100, and 1000 mg/kg at 7-day intervals. Blood pressure, heart rate, and ECG parameters (PR interval, QRS duration, QT interval, and QTc) were measured via a telemetry system (ART/Gold, ver. 4.3, Data Sciences International), which was implanted into the intra-abdominal cavity of animals before dosing; parameters were evaluated 1 and 2 h before dosing, and 1, 2, 4, 7, and 24 h after dosing.

In Vivo Toxicology Studies

Crl:CD1(ICR) mice (*n* = 15/sex/group; 5-weeks-old) or Cynomolgus monkeys (*n* = 4/sex/group; 3–4-years-old) were treated with DS-1971a at 0, 30, 100, and 1000 mg/kg for 6 months, or 0, 10, 100, and 1000 mg/kg for 9 months. In the mouse study, additional animals were used to evaluate TK (*n* = 3 for each blood sampling point), for which they were dosed with the test compounds at the indicated doses. In addition, in the monkey study, additional animals (*n* = 2/sex) were treated with DS-1971a at 1000 mg/kg for 9 months, and were withdrawn from treatment to assess the reversibility of any toxicities following a 1-month recovery period. Animals were euthanized the day after the last dose, and the indicated tissues

and organs were collected to assess organ weight and for histopathological examination. Blood samples were exsanguinated via the abdominal aorta and assayed for serum chemistry.

ACKNOWLEDGMENTS

The authors would like to thank Dr. Makoto Suzuki for the X-ray crystal analysis of DS-1971a.

ASSOCIATED CONTENT

Supporting Information

The Supporting Information is available free of charge on the ACS Publications website at DOI:

Effect of *rac*-**6l**, *rac*-**6o**, and *rac*-**6p** on thermal hyperalgesia in PSL mice

Effect of compound **II** on thermal hyperalgesia in PSL mice

X-ray crystallographic data for DS-1971a

Eurofins lead profiling data for DS-1971a

Plasma DS-1971a concentrations in the PK study on mice (individual data)

Plasma DS-1971a concentrations in the toxicity study on mice (individual data, day 182)

LC-MS trace (PDF)

Molecular formula strings (CSV)

AUTHOR INFORMATION

Corresponding Author

*Tel: +81-70-1440-2862. Fax: +81-3-5436-8561. E-mail: sinozu.xf6@gmail.com; shinozuka.tsuyoshi.s5@daiichisankyo.co.jp.

ORCID ID

Tsuyoshi Shinozuka: 0000-0002-7785-6080

Notes

The authors declare no competing financial interests.

ABBREVIATIONS

Na_V, voltage-gated sodium channel; MBI, mechanism-based inhibition; IDT, idiosyncratic drug toxicity; PSL, partial spinal nerve ligation; NP, neuropathic pain; PNP, peripheral neuropathic pain; DNP, diabetic neuropathic pain; QOL, quality of life; PEPD, paroxysmal extreme pain disorder; PE, peripheral erythromelalgia; CIP, congenital insensitivity to pain; CNS, central nervous system; PNS, peripheral nervous system; CV, cardiovascular; DABCO, 1,4-diazabicyclo[2.2.2]octane; LiHMDS , lithium hexamethyldisilazide; Boc, *tert*-butoxycarbonyl; HLM, human liver microsomes; PWL, paw withdrawal latency; PK, pharmacokinetic; MC, methylcellulose; CL, clearance; V_{ss}, distribution volume; NOEL, no observed effect level; TK, toxicokinetic; NOAEL, no observed adverse effect level.

REFERENCES

(1) Treede, R.-D.; Jensen, T. S.; Campbell, J. N.; Cruccu, G.; Dostrovsky, J. O.; Griffin, J. W.; Hansson, P.; Hughes, R.; Nurmikko, T.; Serra, J. Neuropathic pain. *Neurology* **2008**, *70*, 1630-1635.

(2) Meacham, K.; Shepherd, A.; Mohapatra, D. P.; Haroutounian, S. Neuropathic pain: central vs. peripheral mechanisms. *Curr. Pain Headache Rep.* **2017**, *21*, 28.

(3) Albers, J. W., and Pop-Busui, R. Diabetic neuropathy: mechanisms, emerging treatments, and subtypes. *Curr. Neurol. Neurosci. Rep.* **2014**, *14*, 473.

(4) Dworkin, R. H.; O'Connor, A. B.; Backonja, M.; Farrar, J. T.; Finnerup, N. B.; Jensen, T. S.; Kalso, E. A.; Loeser, J. D.; Miaskowski, C.; Nurmikko, T. J.; Portenoy, R. K.; Rice, A. S.; Stacey, B. R.; Treede, R. D.; Turk, D. C.; Wallace, M. S. Pharmacologic management of neuropathic pain: evidence-based recommendations. *Pain* **2007**, *132*, 237-251.

(5) Fertleman, C. R.; Baker, M. D.; Parker, K. A.; Moffatt, S.; Elmslie, F. V.; Abrahamsen, B.; Ostman, J.; Klugbauer, N.; Wood, J. N.; Gardiner, R. M.; Rees, M. SCN9A mutations in paroxysmal extreme pain disorder: allelic variants underlie distinct channel defects and phenotypes. *Neuron* **2006**, *52*, 767-774.

(6) Yang, Y.; Wang, Y.; Li, S.; Xu, Z.; Li, H.; Ma, L.; Fan, J.; Bu, D.; Fan, Z.; Wu, G.; Jin, J.; Ding, B.; Zhu, X.; Shen, Y. Mutations in SCN9A, encoding a sodium channel alpha subunit, in patients with primary erythermalgia. *J. Med. Genet.* **2004**, *41*, 171-174.

(7) Drenth, J. P.; te Morsche, R. H.; Guillet, G.; Taieb, A.; Kirby, R. L.; Jansen, J. B. SCN9A mutations define primary erythermalgia as a neuropathic disorder of voltage gated sodium channels. *J. Invest. Dermatol.* **2005**, *124*, 1333-1338.

(8) Cox, J. J.; Reimann, F.; Nicholas, A. K.; Thornton, G.; Roberts, E.; Springell, K.; Karbani, G.; Jafri, H.; Mannan, J.; Raashid, Y.; Al-Gazali, L.; Hamamy, H.; Valente, E. M.; Gorman, S.; Williams, R.; McHale, D. P.; Wood, J. N.; Gribble, F. M.; Woods, G. C. An SCN9A channelopathy causes congenital inability to experience pain. *Nature* **2006**, *444*, 894-898.

(9) Goldberg, Y. P.; MacFarlane, J.; MacDonald, M. L.; Thompson, J.; Dube, M. P.; Mattice, M.; Fraser, R.; Young, C.; Hossain, S.; Pape, T.; Payne, B.; Radomski, C.; Donaldson, G.; Ives, E.; Cox, J.; Younghusband, H. B.; Green, R.; Duff, A.; Boltshauser, E.; Grinspan, G. A.; Dimon, J. H.; Sibley, B. G.; Andria, G.; Toscano, E.; Kerdraon, J.; Bowsher, D.; Pimstone, S. N.; Samuels, M. E.; Sherrington, R.; Hayden, M. R. Loss-of-function mutations in the $Na_V1.7$ gene underlie congenital indifference to pain in multiple human populations. *Clin. Genet.* **2007**, *71*, 311-319.

(10) Minett, M. S.; Nassar, M. A.; Clark, A. K.; Passmore, G.; Dickenson, A. H.; Wang, F.; Malcangio, M.; Wood, J. N. Distinct Nav1.7-dependent pain sensations require different sets of sensory and sympathetic neurons *Nature Commun.* **2012**, *3*, 791.

(11) Eijkelkamp, N.; Linley, J. E.; Baker, M. D.; Minett, M. S.; Cregg, R.; Werdehausen, R.; Rugiero, F.; Wood, J. N. Neurological perspectives on voltage-gated sodium channels. *Brain* **2012**, *135*, 2585-2612.

(12) Freeman R, Durso-DeCruz E, Emir B. Efficacy, safety, and tolerability of pregabalin treatment for painful diabetic peripheral neuropathy: findings from seven randomized, controlled trials across a range of doses. *Diabetes Care* **2008**, *31*, 1448-1454.

(13) (a) Schmunk, G.; Gargus, J. J. Channelopathy pathogenesis in autism spectrum disorders. *Front. Genet.* **2013**, *4*, 222. (b) Catterall, W. A.; Goldin, A. L.; Waxman, S. G. International union of pharmacology. XLVII. Nomenclature and structure−function relationships of voltage-gated sodium channels. *Pharmacol. Rev.* **2005**, *57*, 397-409.

(14) Mulroy, M. Systemic toxicity and cardiotoxicity from local anesthetics: Incidence and preventive measures. *Reg. Anesth. Pain Med.* **2002**, *27*, 556-561.

(15) Suzuki, S.; Kuroda, T.; Kimoto, H.; Domon, Y.; Kubota, K.; Kitano, Y.; Yokoyama, T.; Shimizugawa, A.; Sugita, R.; Koishi, R.; Asano, D.; Tamaki, K.; Shinozuka, T.; Kobayashi, H. Discovery of (phenoxy-2-hydroxypropyl)piperidines as a novel class of voltage-gated sodium channel 1.7 inhibitors *Bioorg. Med. Chem. Lett.* **2015**, *25*, 5419-5423.

(16) (a) Swain, N. A.; Batchelor, D.; Beaudoin, S.; Bechle, B. M.; Bradley, P. A.; Brown, A. D.; Brown, B.; Butcher, K. J.; Butt, R. P.; Chapman, M. L.; Denton, S.; Ellis, D.; Galan, S.; Gaulier, S. M.; Greener, B. S.; de Groot, M. J.; Glossop, M. S.; Gurrell, I. K.; Hannam, J.; Johnson, M. S.; Lin, Z.; Markworth, C. J.; Marron, B. E.; Millan, D. S.; Nakagawa, S.; Pike, A.; Printzenhoff, D.; Rawson, D. J.; Ransley, S. J.; Reister, S. M.; Sasaki, K.; Storer, R. I.; Stupple, P. A.; West, C. W. Discovery of clinical candidate 4-[2-(5-Amino-1H-pyrazol-4-yl)-4-chlorophenoxy]-5-chloro-2-fluoro-N-1,3-thiazol-4-ylbenzenesulfonamide (PF-05089771): design and optimization of diaryl ether aryl sulfonamides as selective inhibitors of $Na_V1.7$. *J. Med. Chem.* **2017**, *60*, 7029-7042. (b) Beaudoin, S.; Laufer-Sweiler, M. C.; Markworth, C. J.; Marron, B. E.; Millan, D. S.; Rawson, D. J.; Reister, S. M.; Sasaki, K.; Storer, R. I.; Stupple, P. A.; Swain, N. A.; West, C. W.; Zhou, S. Sulfonamide Derivatives. PCT Int. Appl. WO2010079443, Jul 15, 2010.

(17) (a) McKerrall, S. J.; Nguyen, T.; Lai, K. W.; Bergeron, P.; Deng, L.; DiPasquale, A.; Chang, J. H.; Chen, J.; Chernov-Rogan, T.; Hackos, D. H.; Maher, J.; Ortwine, D. F.; Pang, J.; Payandeh, J.; Proctor, W. R.; Shields, S. D.; Vogt, J.; Ji, P.; Liu, W.; Ballini, E.; Schumann, L.; Tarozzo, G.; Bankar, G.; Chowdhury, S.; Hasan, A.; Johnson, J. P., Jr.; Khakh, K.; Lin, S.; Cohen, C. J.; Dehnhardt, C. M.; Safina, B. S.; Sutherlin, D. P. Structure- and ligand-based discovery of chromane arylsulfonamide

$Na_V1.7$ inhibitors for the treatment of chronic pain. *J. Med. Chem.* **2019**, *62*, 4091-4109. (b) .Luo, G.; Chen, L.; Easton, A.; Newton, A.; Bourin, C.; Shields, E.; Mosure, K.; Soars, M. G.; Knox, R. J.; Matchett, M.; Pieschl, R. L.; Post-Munson, D.; Wang, S.; Herrington, J.; Graef, J.; Newberry, K.; Sivarao, D. V.; Senapati, A.; Bristow, L.; Meanwell, N. A.; Thompson, L. A.; Dzierba, C. D. Discovery of indole- and indazole-acylsulfonamides as potent and selective $Na_V1.7$ inhibitors for the treatment of pain. *J. Med. Chem.* **2019**, *62*, 831-856. (c) Sun, S.; Jia, Q.; Zenova, A. Y.; Wilson, M. S.; Chowdhury, S.; Focken, T.; Li, J.; Decker, S.; Grimwood, M. E.; Andrez, J.-C.; Hemeon, I.; Sheng, T.; Chen, C.-A.; White, A.; Hackos, D. H.; Deng, L.; Bankar, G.; Khakh, K.; Chang, E.; Kwan, R.; Lin, S.; Nelkenbrecher, K.; Sellers, B. D.; DiPasquale, A. G.; Chang, J.; Pang, J.; Sojo, L.; Lindgren, A.; Waldbrook, M.; Xie, Z.; Young, C.; Johnson, J. P.; Robinette, C. L.; Cohen, C. J.; Safina, B. S.; Sutherlin, D. P.; Ortwine, D. F.; Dehnhardt, C. M. Identification of selective acyl sulfonamide-cycloalkylether inhibitors of the voltage-gated sodium channel (Na_V) 1.7 with Potent Analgesic Activity. *J. Med. Chem.* **2019**, *62*, 908-927. (d) Focken, T.; Chowdhury, S.; Zenova, A.; Grimwood, M. E.; Chabot, C.; Sheng, T.; Hemeon, I.; Decker, S. M.; Wilson, M.; Bichler, P.; Jia, Q.; Sun, S.; Young, C.; Lin, S.; Goodchild, S. J.; Shuart, N. G.; Chang, E.; Xie, Z.; Li, B.; Khakh, K.; Bankar, G.; Waldbrook, M.; Kwan, R.; Nelkenbrecher, K.; Tari, P. K.; Chahal, N.; Sojo, L.; Robinette, C. L.; White, A. D.; Chen, C.; Zhang, Y.; Pang, J.; Chang, J. H.; Hackos, D. H.; Johnson, J. P.; Cohen, C. J.; Ortwine, D. F.; Sutherlin, D. P.; Dehnhardt, C. M.; Safina, B. S. Design of conformationally constrained acyl sulfonamide isosteres: identification of *N*-([1,2,4]triazolo[4,3-a]pyridin-3-yl)methane-sulfonamides as potent and selective $hNa_V1.7$ inhibitors for the treatment of pain. *J. Med. Chem.* **2018**, *61*, 4810-4831. (e) Focken, T.; Liu, S.; Chahal, N.; Dauphinais, M.; Grimwood, M. E.; Chowdhury, S.; Hemeon, I.; Bichler, P.; Bogucki, D.; Waldbrook, M.; Bankar, G.; Sojo, L. E.; Young, C.; Lin, S.; Shuart, N.; Kwan, R.; Pang, J.; Chang, J. H.; Safina, B. S.; Sutherlin, D. P.; Johnson, J. P., Jr; Dehnhardt, C. M.; Mansour, T. S.; Oballa, R. M.; Cohen, C. J.; Robinette, C. L. Discovery of aryl sulfonamides as isoform-selective inhibitors of $Na_V1.7$ with efficacy in rodent pain models. *ACS Med. Chem. Lett.* **2016**, *7*, 277-282. (f) Marx, I. E.; Dineen, T. A.; Able, J.; Bode, C.; Bregman, H.; Chu-

Moyer, M.; DiMauro, E. F.; Du, B.; Foti, R. S.; Fremeau, R. T., Jr.; Gao, H.; Gunaydin, H.; Hall, B. E.; Huang, L.; Kornecook, T.; Kreiman, C. R.; La, D. S.; Ligutti, J.; Lin, M.-H. J.; Liu, S.; McDermott, J. S.; Moyer, B. D.; Peterson, E. A.; Roberts, J. T.; Rose, P. E.; Wang, J.; Youngblood, B. D.; Yu, V. L.; Weiss, M. M. Sulfonamides as selective $Na_V1.7$ inhibitors: optimizing potency and pharmacokinetics to enable in vivo target engagement. *ACS Med. Chem. Lett.* **2016**, *7*, 1062-1067. (g) Wu, Y.-J.; Guernon, J.; Shi, J.; Ditta, J.; Robbins, K. J.; Rajamani, R.; Easton, A.; Newton, A.; Bourin, C.; Mosure, K.; Soars, M. G.; Knox, R. J.; Matchett, M.; Pieschl, R. L.; Post-Munson, D. J.; Wang, S.; Herrington, J.; Graef, J.; Newberry, K.; Bristow, L. J.; Meanwell, N. A.; Olson, R.; Thompson, L. A.; Dzierba, C. Development of new benzenesulfonamides as potent and selective $Na_V1.7$ inhibitors for the treatment of pain. *J. Med. Chem.* **2017**, *60*, 2513-2525. (h) Weiss, M. M.; Dineen, T. A.; Marx, I. E.; Altmann, S.; Boezio, A. A.; Bregman, H.; Chu-Moyer, M. Y.; DiMauro, E. F.; Feric Boijic, E.; Foti, R. S.; Gao, H.; Graceffa, R. F.; Gunaydin, H.; Guzman-Perez, A.; Huang, H.; Huang, L.; Jarosh, M.; Kornecook, T.; Kreiman, C. R.; Ligutti, J.; La, D. S.; Lin, M.-H. J.; Liu, D.; Moyer, B. D.; Nguyen, H. N.; Peterson, E. A.; Rose, P. E.; Taborn, K.; Youngblood, B. D.; Yu, V. L.; Fremeau, R. T., Jr. Sulfonamides as selective $Na_V1.7$ inhibitors: optimizing potency and pharmacokinetics while mitigating metabolic liabilities. *J. Med. Chem.* **2017**, *60*, 5969-5989. (i) Wu, W.; Li, Z.; Yang, G.; Teng, M.; Qin, J.; Hu, Z.; Hou, L.; Shen, L.; Dong, H.; Zhang, Y.; Li, J.; Chen, S.; Tian, J.; Zhang, J.; Ye, L. The discovery of tetrahydropyridine analogs as $hNa_V1.7$ selective inhibitors for analgesia. *Bioorg. Med. Chem. Lett.* **2017**, *27*, 2210-2215. (j) Graceffa, R. F.; Boezio, A. A.; Able, J.; Altmann, S.; Berry, L. M.; Boezio, C.; Butler, J. R.; Chu-Moyer, M.; Cooke, M.; DiMauro, E. F.; Dineen, T. A.; Feric Bojic, F.; Foti, R. S.; Fremeau, R. T., Jr.; Guzman-Perez, A.; Gao, H.; Gunaydin, H.; Huang, H.; Huang, L.; Ilch, C.; Jarosh, M.; Kornecook, T.; Kreiman, C. R.; La, D. S.; Ligutti, J.; Milgram, B. C.; Lin, M.-H. J.; Marx, I. E.; Nguyen, H. N.; Peterson, E. A.; Rescourio, G.; Roberts, J.; Schenkel, L.; Shimanovich, R.; Sparling, B. A.; Stellwagen, J.; Taborn, K.; Vaida, K. R.; Wang, J.; Yeoman, J.; Yu, V.; Zhu, D.; Moyer, B. D.; Weiss, M. M. Sulfonamides as selective $Na_V1.7$ inhibitors: optimizing potency, pharmacokinetics, and metabolic properties to obtain atropisomeric quinolinone (AM-0466)

that affords robust in vivo activity. *J. Med. Chem.* **2017**, *60*, 5990-6017. (k) Storer, R. I.; Pike, A.; Swain, N. A.; Alexandrou, A. J.; Bechle, B. M.; Blakemore, D. C.; Brown, A. D.; Castle, N. A.; Corbett, M. S.; Flanagan, N. J.; Fengas, D.; Johnson, M. S.; Jones, L. H.; Marron, B. E.; Payne, C. E.; Printzenhoff, D.; Rawson, D. J.; Rose, C. R.; Ryckmans, T.; Sun, J.; Theile, J. W.; Torella, R.; Tseng, E.; Warmus, J. S. Highly potent and selective $Na_V1.7$ inhibitors for use as intravenous agents and chemical probes. *Bioorg. Med. Chem. Lett.* **2017**, *27*, 4805-4811.

(18) McDonnell, A.; Collins, S.; Ali, Z.; Iavarone, L.; Surujbally, R.; Kirby, S.; Butt, R. P. Efficacy of the Nav1.7 blocker PF-05089771 in a randomised, placebo-controlled, double-blind clinical study in subjects with painful diabetic peripheral neuropathy. *Pain* **2018**, *159*, 1465-1476.

(19) The existence of hydrophobic floor to interact with this phenyl ring is shown, see: Ahuja, S.; Mukund, S.; Deng, L.; Khakh, K.; Chang, E.; Ho, H.; Shriver, S.; Young, C.; Lin, S.; Johnson, J. P.; Wu, P.; Li, J.; Coons, M.; Tam, C.; Brillantes, B.; Sampang, H.; Mortara, K.; Bowman, K. K.; Clark, K. R.; Estevez, A.; Xie, Z.; Verschoof, H.; Grimwood, M.; Dehnhardt, C.; Andrez, J.-C.; Focken, T.; Sutherlin, D. P.; Safina, B. S.; Starovasnik, M. A.; Ortwine, D. F.; Franke, Y.; Cohen, C. J.; Hackos, D. H.; Koth, C. M.; Payandeh, J. Structural basis of Nav1.7 inhibition by an isoform-selective small-molecule antagonist. *Science* **2015**, *350*, aac5464.

(20) Yan, Z.; Caldwell, G. W. Stable-isotope trapping and high-throughput screenings of reactive metabolites using the isotope MS signature. *Anal. Chem.* **2004**, *76*, 6835-6847.

(21) Seltzer, Z.; Dubnerb, R.; Shirc, Y. A novel behavioral model of neuropathic pain disorders produced in rats by partial sciatic nerve injury *Pain* **1990**, *43*, 205-218.

(22) The pharmacological results are reported in Supporting Information.

(23) Eurofin's Pan Labs lead profiling screen. This battery of radioligand binding assays consists of 67 common GPCRs, ion channels, and transporters, see Supporting Information for complete results.

(24) Kim, S. H.; Chung, J. M. An experimental model for peripheral neuropathy produced by segmental spinal nerve ligation in the rat *Pain* **1992**, *50*, 355-363.

(25) Fukuoka, T.; Kobayashi, K.; Yamanaka, H.; Obata, K.; Dai, Y.; Noguchi, K. Comparative study of the distribution of the alpha-subunits of voltage-gated sodium channels in normal and axotomized rat dorsal root ganglion neurons *J. Comp. Neurol.* **2008**, *510*, 188-206.

(26) Copeland, R. A.; Pompliano, D. L.; Meek, T. D. Drug−target residence time and its implications for lead optimization *Nat. Rev. Drug Discovery* **2006**, *5*, 730-739.

(27) Shinozuka, T.; Tsukada, T.; Fujii, K.; Tokumaru, E.; Matsui, Y.; Wakimoto, S.; Ogata, T.; Araki, K.; Sawamura, R.; Watanabe, N.; Mori, M.; Tanaka J. Structure−activity relationship studies of 3- or 4‑pyridine derivatives of DS-6930 *ACS Med. Chem. Lett.* **2019** *10*, 358-362.

(28) Yoshikawa, K.; Yokomizo, A.; Naito, H.; Haginoya, N.; Kobayashi, S.; Yoshino, T.; Nagata, T.; Mochizuki, A.; Osanai, K.; Watanabe, K.; Kanno, H.; Ohta, T. Design, synthesis, and SAR of cis-1,2-diaminocyclohexane derivatives as potent factor Xa inhibitors. Part I: Exploration of 5−6 fused rings as alternative S1 moieties. *Bioorg. Med. Chem.* **2009**, *17*, 8206-8220.

(29) Nagata, T.; Yoshino, T.; Haginoya, N.; Yoshikawa, K.; Nagamochi, M.; Kobayashi, S.; Komoriya, S.; Yokomizo, A.; Muto, R.; Yamaguchi, M.; Osanai, K.; Suzuki, M.; Kanno, H. Discovery of *N*-[(1R,2S,5S)-2-{[(5-chloroindol-2-yl)carbonyl]amino}-5-(dimethylcarbamoyl)cyclohexyl]-5-methyl-4,5,6,7-tetrahydrothiazolo-[5,4-c]pyridine-2-carboxamide hydrochloride: A novel, potent and orally active direct inhibitor of factor Xa. *Bioorg. Med. Chem.* **2009**, *17*, 1193-1206.

(30) Watanabe, A.; Nakamura, K.; Okudaira, N.; Okazaki, O. Sudo. K. Risk assessment for drug-drug interaction caused by metabolismbased inhibition of CYP3A using automated in vitro assay systems and its application in the early drug discovery process. *Drug Metab. Dispos.* **2007**, *35*, 1232-1238.

(31) Ogiyama, T.; Yamaguchi, M.; Kurikawa, N.; Honzumi, S.; Yamamoto, Y.; Sugiyama, D.; Takakusa, H.; Inoue S. Identification of a novel hormone sensitive lipase inhibitor with a reduced potential of reactive metabolites formation. *Bioorg Med Chem.* **2017**, *25,* 2234-2243.

(32) Irwin, S. Comprehensive observational assessment: 1a. A systematic, quantitative procedure for assessing the behavioral and physiologic state of the mouse *Psychopharmacologia (Berl.)* **1968**; *13*, 222-257.

TABLE OF CONTENTS GRAPHIC

Discovery of DS-1971a, a Potent Selective $Na_V1.7$ Inhibitor

Tsuyoshi Shinozuka,*,† Hiroyuki Kobayashi,† Sayaka Suzuki,† Kyosuke Tanaka,† Narayan Karanjule,† Noriyuki Hayashi,† Toshifumi Tsuda,† Eri Tokumaru,† Masahiro Inoue,† Kiyono Ueda,‡ Hiroko Kimoto,† Yuki Domon,† Sakiko Takahashi,† Kazufumi Kubota,† Tomihisa Yokoyama,† Akiko Shimizugawa,† Ryuta Koishi,‡ Daigo Asano,† Tomoko Sakakura,† Kiyoshi Takasuna,† Yasuyuki Abe,† Toshiyuki Watanabe,† and Yutaka Kitano†